CAD Enabling Smart Handtools

by

Pragun Goyal

Submitted to the Program in Media Arts and Sciences,
School of Architecture and Planning,
in partial fulfillment of the requirements for the degree of

Master of Science in Media Arts and Sciences

at the

MASSACHUSETTS INSTITUTE OF TECHNOLOGY

September 2014

Signature redacted

Author ....
Program in Media Arts and Sciences,
School of Architecture and Planning,
August 8, 2014

Signature redacted

Certified by............. ....
Joseph A. Paradiso
Associate Professor of Media Arts and Sciences
Program in Media Arts and Sciences
Thesis Supervisor

Signature redacted

Accepted by ....
Prof. Patricia Maes
Interim Department Head
Program in Media Arts and Sciences

CAD Enabling Smart Handtools

by

Pragun Goyal

Submitted to the Program in Media Arts and Sciences,
School of Architecture and Planning,
on August 8, 2014, in partial fulfillment of the
requirements for the degree of
Master of Science in Media Arts and Sciences

Abstract

CAD (Computer Aided Design) software allows one to describe a design in great detail and at any arbitary scale. However, our interface to CAD is still largely through traditional avenues: screen, keyboard and pointing devices. While these interfaces function for their intended purposes: text entry, pointing, browsing, etc, they are not designed for the purpose of mediating the flow of information from and to a physical workpiece. Traditional input interfaces are limited in the sense that they lack a direct connection with the workpiece, forcing the user to translate information gathered from the workpiece before it can be input into the computer. A similar disconnect also exists in the realm of output from the computer. On one extreme, the screen as an output interface forces the user to interpret and translate information conveyed graphically to the context of the workpiece at hand. On the other extreme, devices like CNC machines and 3D printers lack a way for the user to engage with the fabrication and to iteratively change design parameters in realtime.

In this work, I present, two handtools that build on the philosophy of Free-D ([1] and [2]), a smart milling tool recently developed in our research group. to create a similar interface between Computer Aided Design and the physical workpiece, in entirely different application domains. The two handtools are BoardLab and Nishanchi. BoardLab is a smart, context-aware oscilloscope probe that can be used to dynamically search for just-in-time information on electronic circuit board design data and to automatically annotate the design data with measurements and test data. Nishanchi is a handheld inkjet printer and 3D digitizer that can be used to print raster graphics on non-conformable surfaces.

Thesis Supervisor: Joseph A. Paradiso
Title: Associate Professor of Media Arts and Sciences
Program in Media Arts and Sciences

The following people served as readers for this thesis:

Signature redacted

Thesis Reader ....

Prof. Patricia Maes
Alexander W. Dreyfoos (1954) Professor
Program in Media Arts and Sciences

Signature redacted

Thesis Reader .. ..

Amit Zoran
Post-doctoral Associate
Fluid Interfaces Group
Program in Media Arts and Sciences

Acknowledgments

I am thankful to Prof. Joe Paradiso, Amit Zoran and Prof. Pattie Maes for their feedback as readers. Thanks to Amit for helping me develop my own understanding of the role that technolgy plays in our lives and for always giving me insightful design critique on my work. Thanks to my parents, Isha, Lina, Amna and Anirudh for moral support and encouragement. Special thanks to Lina for help in making this thesis so much more understandable and cleanly written. I am thankful to my parents, Isha and Wooly for tolerating my long absence from home while I was pursuing the work in this thesis.

Contents

List of Figures

Chapter 1

Introduction

An excellent survey of smart tools is given in [3]; here I highlight a few particular examples to stimulate the discussion. SketchPad [4] was probably one of the first applications of computing to create, edit, and store graphic designs. Now, CAD (Computer Aided Design) softwares allows one to describe a design in great detail and at varying scales. However, the interaction with CAD software is still largely through traditional interfaces: screen, keyboard and pointing devices. While these interfaces function for their intended purposes – text entry, pointing, browsing, etc. They are not designed for the purpose of mediating the flow of information from and to a physical workpiece. Traditional input interfaces are limited in the sense that they lack a direct connection with the workpiece, forcing the user to translate information gathered from the workpiece before it can be input into the computer. A similar disconnect also exists in the realm of output from the computer. On one extreme, the screen as an output interface forces the user to interpret and translate information conveyed graphically to the context of the workpiece at hand. On the other extreme are devices like CNC machines and 3D printers – while these devices maintain a high-bandwidth connection with the workpiece, they completely lack a way for the user to engage with the fabrication and to iteratively change design parameters in realtime.

Handtools have been traditionally used throughout the history of mankind for fabrication. A traditional handtool acts as an interface between the user and the workpiece. Inspired by Free-D [1] and [2], which acts as an adaptive interface between the computer, the user and the workpiece, I present, two handtools that build on the philosophy of Free-D to bring a seamless interface between Computer Aided Design and the physical workpiece to these applications. The two handtools are BoardLab and Nishanchi. BoardLab is a smart context-aware oscilloscope probe that can be used to search for just-in-time information of electronic circuit board design data and to annotate the design data with measurements and test data, both dependent on the circuit element or node being probed. Nishanchi is a handheld inkjet printer and 3D digitizer that can be used to print raster graphics on non-conformable surfaces.

In both projects, the position and orientation of the tool is tracked with respect to the workpiece. A computer uses the tool position and orientation with a CAD model of the workpiece and actuates the tool automatically depending on the mode of operation and user-triggered events. This allows for the user and the handtool to interact with the workpiece in a tight choreography, leveraging craft skills as when exploiting a conventional handtool, while still maintaining a realtime connection with the computer model of the workpiece.

1.1 Related Work

There have been a number of smart tools built for different specific applications. The Wacom tablet and pen [5], and the Anoto digital pen [6] allow the user to write on paper while digitizing the input at the same time. The flow of information in these tools is mainly from the workpiece to the computer. Kim et al. present a way of using a computer controlled pencil to allow the user to create sketches on paper [7]. Junichi et al. present another approach to a hybrid pen-paper interaction where the tip of the pen is actuated by computer controlled magnets [8]. These tools demonstrate how, within the realm of sketching using pen/pencils, a handtool can mediate the flow of information from the computer to the workpiece and vice versa.

The same philosophy is exemplified in the realm of painting and digital painting by I/O Brush [9], Fluidpaint [10] and Intupaint [11]. I/O Brush uses images and videos taken at a close range from everyday objects to create a final graphic. Fluidpaint and Intupaint allow the use of conventional brushes in digital medium. Baxter et al. simulate the forces felt while brushing using actuation to allow users to express themselves creatively in the digital painting medium [12]. These tools allow the user to be much more expressive in painting in the digital medium; however, it is not clear how the digital medium aids the user in the creation of a physical artifact.

In the realm of 3D object creation, tools like the Creaform 3D Handheld Scanner [13] allow the user to create a 3D model of an existing workpiece. Song et al. describe an approach in which annotation marks made on the workpiece instruct changes to a computer 3D model [14]. However, in these approaches, the tool does not help in translating the changes expressed on the computer back to the workpiece.

My work is closest in spirit to Free-D ([1] and [2]), and the work done by Rivers et al. [15]. However, one of the key difference is that both BoardLab and Nishanchi are designed to work with existing semi-complete or complete artifacts. In the case of Boardlab, a description of the electronic circuit is loaded into the software in the form of the PCB layout and the schematic data. In the case of Nishanchi, the digitizing tip allows the user to input relevant parameters about the workpiece into the CAD software. The projects also differ from ([1], [2] and [15]) in that the output of the tool is in the form of design information rather than a fabricated workpiece.

Chapter 2

BoardLab

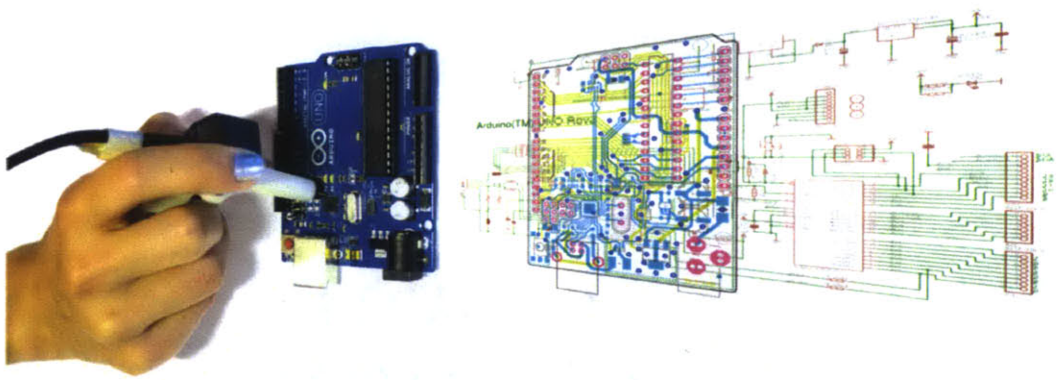

Figure 2-1: BoardLab conceptual diagram

2.1 Introduction

Use of Electronic Design Automation (EDA) software has become quite popular in the design of Printed Circuit Boards (PCBs). A very common paradigm is to design the schematics first and then convert them to a PCB layout. The resulting PCB layout can then be fabricated and assembled with electronic components. Access to the schematic design data of a PCB is quite helpful while testing and assembling a PCB, because such data gives the user a good idea of how the components are connected. This becomes even more important while debugging a PCB or while diagnosing a PCB's faults.

A typical electronics workspace. Notice the two displays in front of the user that display schematic diagrams and the PCB layout.

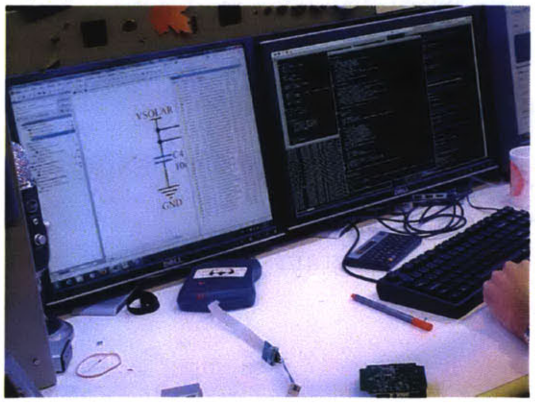
The screen on the left is being used to display schematics and the screen on right to display source code.

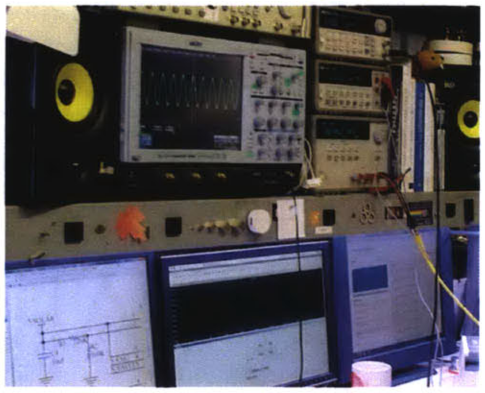
Other screens in the workspace: oscilloscope and multimeters.

Figure 2-2

Although production testing of commercial scale PCBs generally employs a custom made multi-wire probe that automatically engages strategic testpoints on the board. The boards are usually extensively manually probed while being tested and debugged, as in fig 2-2.

While most modern EDA software offers an easy-to-use WYSIWYG (What You See Is What You Get) interface, the keyboard and mouse interface required to query and annotate design data on EDA software creates a disconnect in the workflow of manually debugging or testing a PCB. This is because most operations and tools used in this process involve working directly with the circuit board and its components. However, in order to locate a component in the schematic or in the PCB layout, the user has to try to find a visually similar pattern in the PCB layout file, or else key in the identifier for the component read from the PCB silkscreen annotation. Both of these processes are cumbersome and lead to unnecessary cognitive load. Fig 2-2 shows a photograph of a typical electronics design and prototyping workspace with two display screens dedicated to displaying the schematics and PCB layout, respectively, plus another showing real-time waveforms from the node being probed. Small component sizes and similar looking components further magnify the associated confusion.

Experienced electronics designers often partially work their way around this by annotating the board with design data, including descriptors, part-numbers, component values, etc. However, the board space limits the amount of design information that can be embedded in the annotations. Also, this approach does not work well for denser electronic circuits.

The BoardLab system consists of a handheld probe that allows for direct interaction with the board and board components for just-in-time information on board schematics, component datasheets, and source code. It can also take voltage measurements, which are then annotated on the board schematics. The emphasis is on providing the same kind of interaction with the PCB as is afforded by other commonly used tools, like soldering irons, multimeters, oscilloscopes, etc. Figure 2-1 illustrates how the BoardLab System becomes a way to introspect and annotate the design data using the actual circuit board as the interface. The system supports the following modes:

1. Board positioning mode
2. Component selection mode

3. Voltage annotation mode
4. Waveform verification mode

These different modes are detailed in the following sections.

2.2 Related work

Previous work to provide just-in-time information about electronic circuits involves the use of tagged components, enabling their positions to be tracked in the circuit [16]. However, this technique requires specially constructed components. BoardLab builds on the high-level approach described in [17], where pointing gestures are used to index information tagged with different objects. BoardLab uses a handtool form factor, which allows for pointing at small components on a circuit more accurately. The design of BoardLab has been inspired and informed by the design of of FreeD [2], where a position-orientation tracked handtool provides for interaction with both the physical work piece and the design data at the same time. This approach is also similar to the one described by Rosenberg et al. in [18], where a position-orientation tracked probe is used to verify component positions on a circuit board. The difference, however, is the reuse of design information for the board, which allows for further extension into signal verification and code-introspection.

2.3 Design and technology

Boardlab is designed to be used just like other standard benchtop electronics instrumentation. The user employs a handheld probe to introspect and to make measurements on the circuit board. A computer runs the BoardLab software and displays the results on a screen. A tracking system tracks the position and orientation of the probe as the user engages it. As essentially all modern PCBs are generated in an ECAD system that generates a precise mechanical model of the circuit board, node, trace and component placement can be straightforwardly input to BoardLab.

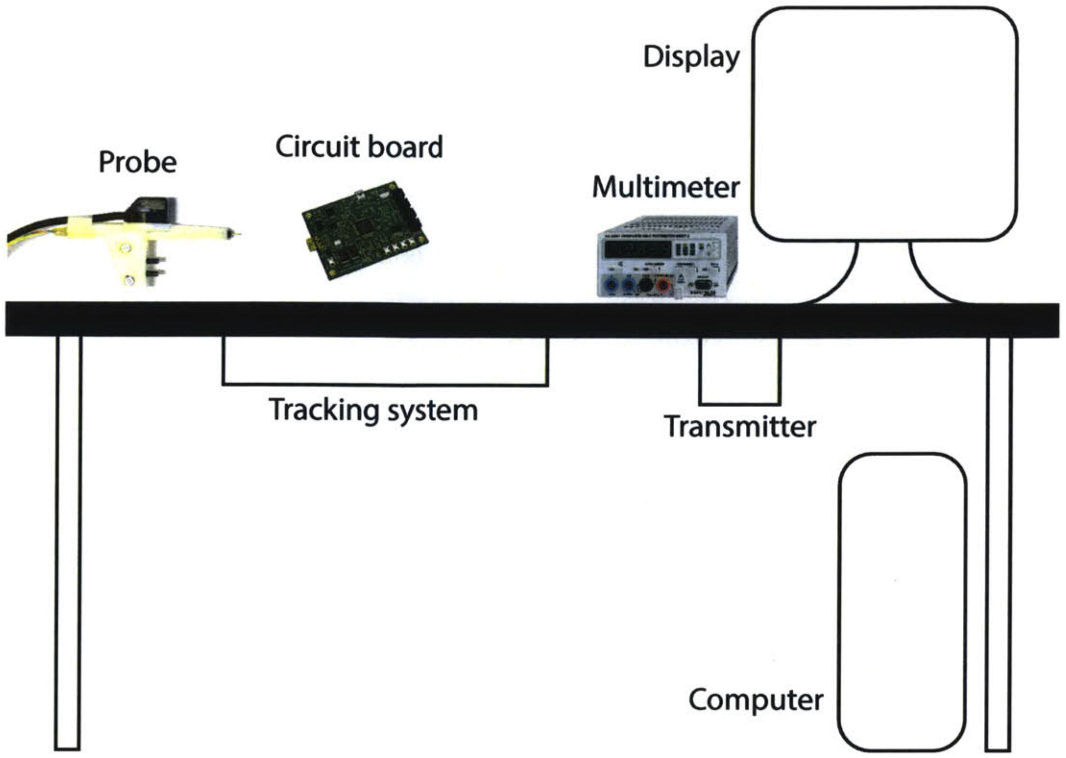

Figure 2-3: An overview of the Boardlab system

2.3.1 Tracking system

The handheld probe is augmented with a MMTS (magnetic motion tracking system) sensor that allows for tracking of the 3D position and 3D orientation of the probe. A Polhemus FASTRAK system (an AC 6D magnetic tracking system [19]) is used to estimate the 3D position and 3D orientation of the probe using a sensor mounted on the probe. The position and orientation state given by the tracking system is translated to get the position of the tip in the reference frame of the workbench. The Polhemus system can be configured to output the orientation data as a quaternion. The following equation is used to get the position of the tip ($\vec{r}_{tip,tx,tx}$) with respect to the transmitter (tx), in the reference frame of the transmitter (tx).

$$\vec{r}_{tip,tx,tx} = \vec{r}_{rx,tx,tx} + M * \vec{r}_{tip,rx,rx} \tag{2.1}$$

where $\vec{r}_{tip,rx,rx}$ is the vector from the receiver (rx) on the probe to the tip (tip) of the probe in probe reference system (rx), and M is the 3x3 rotation matrix derived from the orientation quaternion given by the tracking system.

While the CAD design of the probe could be used to compute the vector that connects the sensor origin to the tip's endpoint, I found that because of 3D printing tolerances and slight misalignment of the sensor on the probe, it is better to calibrate for the vector. The following procedure is used to collect calibration data:

1. The tip of the probe is held fixed to a via (e.g. through-hole) in the board.
2. The probe is moved around making sure that the tip is always touching the via.

Assuming that the sensor is rigidly mounted on the probe, and ignoring the small movement of the tip within the via, the resulting set of position points should lie on the sphere centered at the via and with a radius equal to the vector ($\vec{r}_{tip,rx}$). The center (*center*) and radius ($\vec{r}_{tip,rx}$) of the sphere can be found by importing the point cloud in a CAD program (Rhinocerous) and fitting a sphere to the points. The radius given by the CAD program is the modulus of the vector needed to be computed for calibration. The following equation gives the the r^i_{tx} for point i in the pointcloud in the reference frame of the transmitter (tx). However, as we have the orientation information for each point, we can apply the inverse of the rotation matrix derived from the orientation quaternion for each point to get the $\vec{r}^i_{rx}$. The following equation illuminates the way.

$$r^i_{tip,rx} = M^{-1,i} * r^i_{rx} \tag{2.2}$$

The mean $\vec{r}^i_{tip,rx}$ for all i gives the calibration $\vec{r}_{tip,rx}$. I found that applying a linear RANSAC (RANdom SAmple Consensus) filter to the pointcloud eliminates erroneous data that could be introduced by accidentally moving the probe out of the via during calibration data collection.

2.3.2 PCB layout digestor

The PCB layout digestor, as the name suggests, is the pythonic entity responsible for parsing of the PCB layout file for the circuit board, and to track the projected position of the probe tip on the PCB layout. Needless to say the PCB layout also has to deal with errands like understanding what orientation and position the PCB is placed at on the workbench. The following section describes the position and orientation estimation of the PCB.

PCB position estimation

Given that most electronic circuit boards are rigid and planar, it is relatively safe to assume that the PCB is of planar geometry. We can estimate the 3D position and orientation of the PCB by using the probe tip to estimate the 3D positions of three or more known vias on the PCB. For the sake of completion and intellectual stimulation, the implementation of the algorithm as originally described in [20] is detailed below.

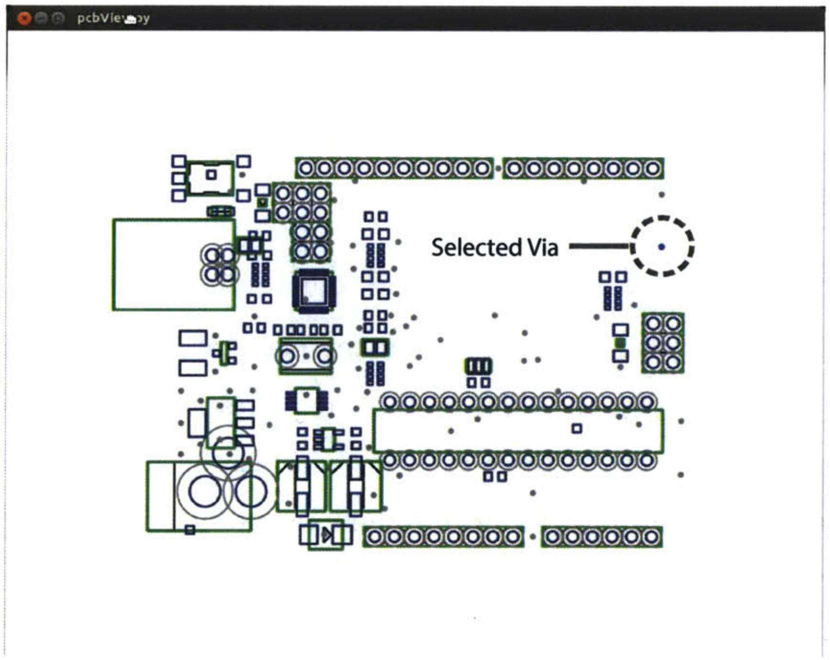

Figure 2-4: The PCB digester highlights the via selected for PCB positioning

The following procedure is used to collect PCB position estimation data:

1. The software picks three (or more) pre-defined vias (Figure 2-4).

2. The user respectively pushes the tip into the via and holds the probe in that position for about 5-7 seconds. The system collects the estimated position data for the probe tip as this is done.

While the PCB position and orientation could be described as a 3D position and 3D orientation, as the PCB features are described as 2D features on the PCB plane, it seemed appropriate to represent the PCB position and orientation as a 2D object on a 3D plane. This would allow the positions of the features of the PCB to be used in their native reference system.

The 3D plane (P_{tx}) is found in the reference frame of the transmitter using a simple least squares fit on the via position data. However, this plane is still represented in the frame of the transmitter. We need to find a reference frame such that one of the major planes of the reference frame is co-planar with the PCB plane; this allows us to move from 3D position to 2D position on the PCB plane by the means of a simple transformation. In order to do that, we need to find three orthonormal unit vectors $ThreeMusketeers$ such that two of them lie in the PCB plane. The following technique is used to find three orthonormal basis vectors.

1. Let $At\vec{h}os$, $Arta\vec{g}nan$ be two of the three lines formed between the three vias selected for calibration. $At\vec{h}os$ forms the first of the three orthonormal unit vectors.

2. $Pat\vec{h}os = At\vec{h}os \times Arta\vec{g}nan$ gives $Pat\vec{h}os$, the second element of $ThreeMusketeers$.

3. The third element of $Arh\vec{e}mis$ is found to be $Pat\vec{h}os \times At\vec{h}os$.

Notice, that $At\vec{h}os$ and $Arh\vec{e}mis$ are in the plane of the PCB, and $Pat\vec{h}os$ is normal to it. Also note that the three vectors are represented in the reference frame of the transmitter. Any of the three arbitrary vias can be selected as the origin of the new reference frame $\vec{r}_{luckyvia,tx}$. Now, the representation of a position of a point p in this new reference frame can be computed as

$$\vec{R}_{p,ThreeMusketeers} = \left[At\vec{h}os, Pat\vec{h}os, Arh\vec{e}mis\right] \times \left(\vec{R}_{p,tx} - \vec{r}_{luckyvia,tx}\right) \tag{2.3}$$

Further, for points on the PCB plane, the component corresponding to $Pat\vec{h}os$ can be dropped, giving us a convenient 2D representation. However, we still need to compensate for the scale, translation, and rotation between the PCB layout 2D frame of reference *pcb* and the 2D frame of reference fixed on the PCB plane: $twoMusketeers$.

Let the $r^i_{twoMusketeers}$ be the position of a via in the *twoMusketeers*, and r^i_{pcb} be the corresponding position in the PCB layout. The scaling can be obtained by simply comparing the mean distances between vias in both frames of reference,

$$scale = \frac{\sum_{i,j\in(1,2,3),i\neq j}\left(|\vec{r^i_{pcb}} - \vec{r^j_{pcb}}||\right)}{\sum_{i,j\in(1,2,3),i\neq j}\left(|\vec{r^{i,mean}_{twoMusketeers}} - \vec{r^{j,mean}_{twoMusketeers}}|)\right)}, \tag{2.4}$$

where $\vec{r^{i,mean}_{twoMusketeers}}$, is the mean of all position estimates for via i.

The translation $r_{\vec{fix}}$ is obtained as the translation between the centroids of the scaled estimated position pointclouds and PCB layout via position pointclouds. The centroid for the pointcloud can be computed as:

$$r_{\vec{fix}} = \vec{r^{centroid}_{pcb}} - scale * \vec{r^{centroid}_{twoMusketeers}} \tag{2.5}$$

The centroids can be found using the following equation:

$$\vec{r^{centroid}} = \frac{\sum_{i=1}^{n}\vec{r^i}}{n} \tag{2.6}$$

The rotation can be obtained as follows:

1. Compute vectors for each via position centered around the centroid.

$$\vec{a^i} = \vec{r^i_{pcb}} - \vec{r^{centroid}_{pcb}}, \tag{2.7}$$

and

$$\vec{b^i} = scale * (\vec{r^i_{twoMusketeers}} - \vec{r^{centroid}_{twoMusketeers}}), \tag{2.8}$$

2. Compute the 2×2 covariance matrix as:

$$S = XIY^T \tag{2.9}$$

where, X, Y are $2 \times n$ matrices with a^i and b^i as their columns. I is a 2×2 identity matrix.

3. Compute the singular value decomposition $S = U\sum V^T$. The 2D rotation matrix is then obtained as:

$$R = VU^T \tag{2.10}$$

At the end of PCB position estimation, the three parameters that define the position and orientation of the PCB are *scale*, r_{fix}, and R. Of course, the board needs to be rigidly held relative to the workbench during the process, otherwise another calibration needs to be performed. Conversly, another tracking device can be rigidly mounted to the board as well although with the Polhemus system, care needs to be taken of distortion from connections or ferros material in proximity to the sensors and EMI.

2.3.3 Probe tip projection on the PCB

The previously described values *scale*, r_{fix}, and R are used to project the probe tip position along the probe vector onto the PCB plane. The projected point is then transformed to the PCB layout reference system.

1. The projection of the probe tip on the PCB plane along the probe vector is:

$$\vec{R_{tx}^{projected}} = \vec{R_{tx}^{tip}} - ((\vec{R_{tx}^{tip}} - \vec{R_{tx}^{origin}}) \cdot Pat\vec{h}os_{tx})Pat\vec{h}os_{tx}, \tag{2.11}$$

where $\vec{R_{tx}^{projected}}$ is the projected point and $\vec{R_{tx}^{origin}}$ is the origin of the PCB plane, both expressed in the reference frame of the transmitter tx.

2. The $\vec{R_{tx}^{projected}}$ is transformed to the $threeMusketeers$ frame of reference $\vec{R_{threeMusketeers}^{projected}}$ using equation 2.3.

3. The $Pat\vec{h}os$ component of $\vec{R_{threeMusketeers}^{projected}}$ is dropped to obtain the 2D point $\vec{R_{twoMusketeers}^{projected}}$ on the PCB plane.

4. The $\vec{R_{twoMusketeers}^{projected}}$ is transformed to PCB layout reference frame $\vec{R_{pcb}}$ by applying the *scale*, r_{fix} and R as computed in the previous subsection, as,

$$\vec{R_{pcb}^{projected}} = R\left(scale * (\vec{R_{twoMusketeers}^{projected}} - \vec{R_{twoMusketeers}^{centroid}})\right) + \vec{R_{pcb}^{centroid}} \tag{2.12}$$

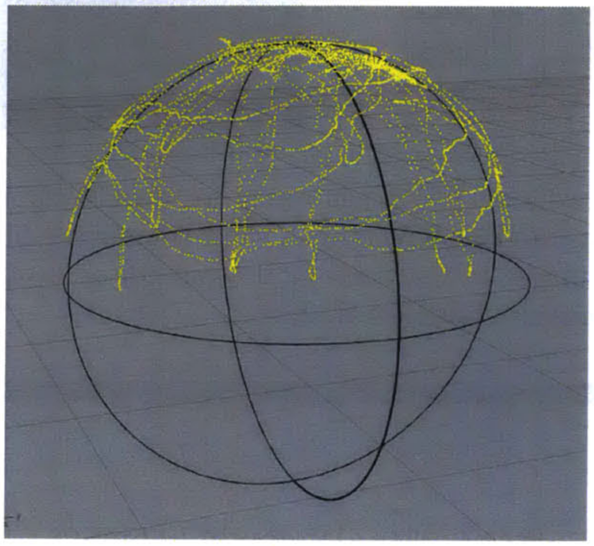
Figure 2-5: Pointcloud for sensor positions while the probe pin is fixed at a via (the center of the sphere)

PCB Feature map

The system supports two types of PCB features: components and pins. For both types of features, maximum rectangular extents are computed based on the PCB top and bottom trace layers and are mapped to active GTK+ widgets. In the event of a probe event, the PCB coordinates of the probe tip projection are checked against the extents of all features of the PCB to find which feature to delegate the probe event to.

2.3.4 The rest of the system

A HP-34401A desktop multimeter is used to provide voltage measurements to annotate the schematics. The SCPI (Standard Command for Programmable Instruments) interface is used to communicate with the multimeter. [21] describes the interface in more detail.

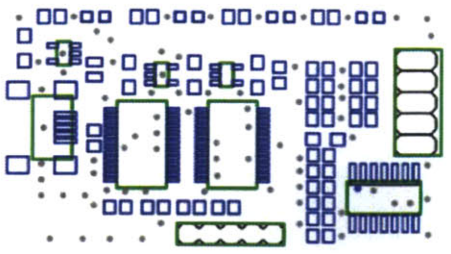
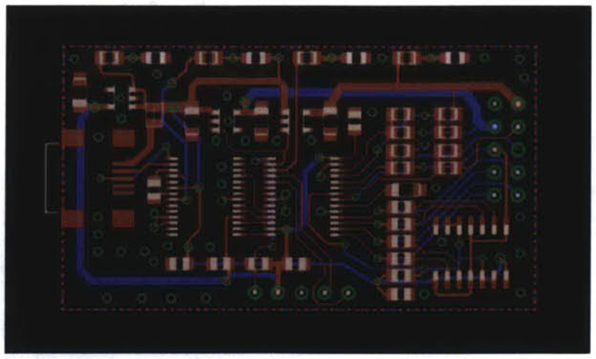

Figure 2-6: Left: BoardLab PCB feature map for a PCB layout. Green rectangles show PCB components, and blue rectangles show component pins. Right: The same PCB layout file as displayed in the Eagle 6.0 Layout editor. Notice the more pleasing and legible color scheme used in BoardLab :)

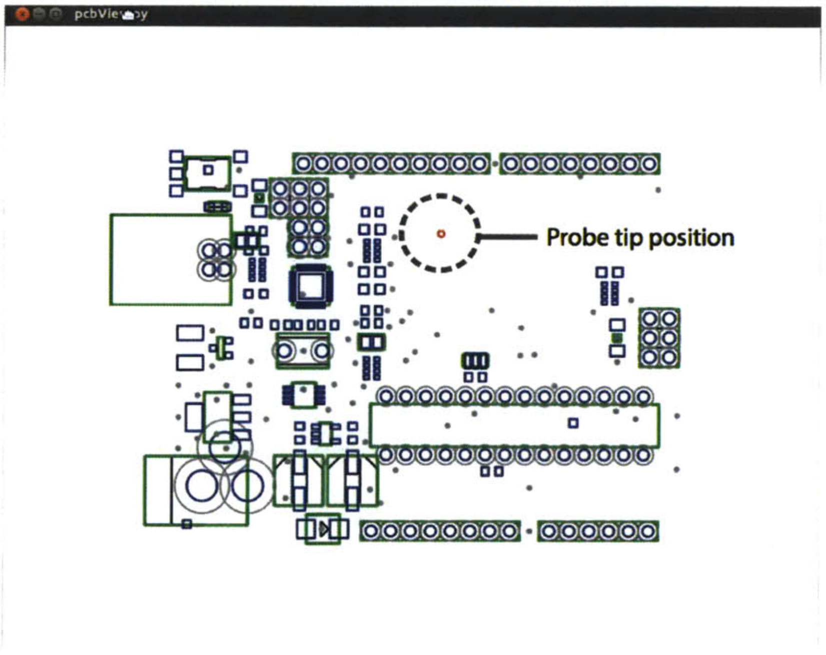

Figure 2-7: The probe position tracked on the PCB feature map

The probe (Figure 2-9) has a conductive metal tip, which is connected to the positive terminal on a desktop multimeter to make measurements. The probe tip is mounted on a spring loaded switch, which closes when the probe is pressed onto the board. The probe has another switch that can be used to cycle through different modes of operation when pressed by the thumb. The switches are connected to an Arduino microcontroller board programmed as a USB HID device. The Arduino

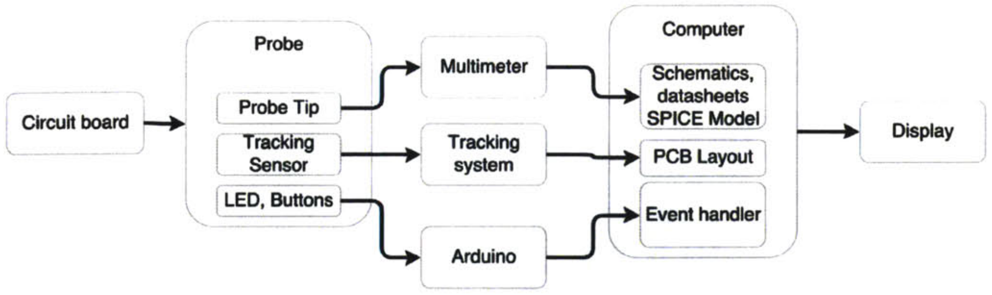

Figure 2-8: Diagram showing how different parts of the BoardLab system are connected.

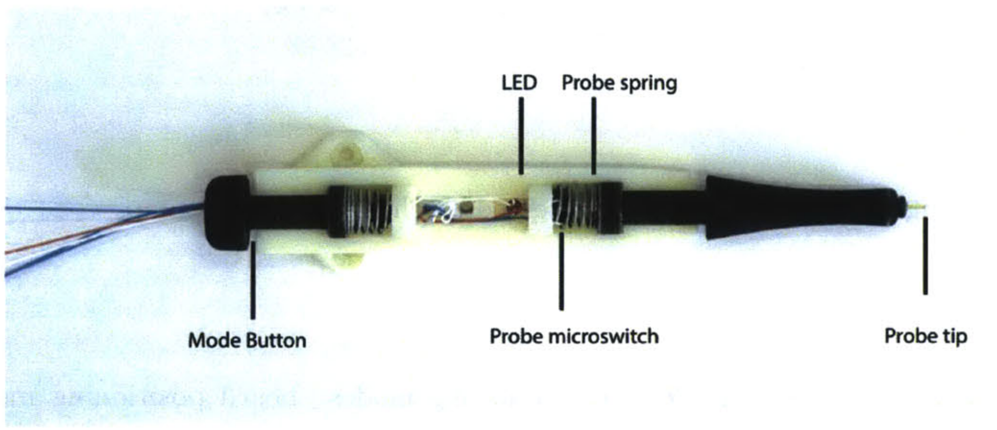

Figure 2-9: The final version of the probe disassembled to show internal assembly

generates computer keyboard events for switch events on the probe. The probe also has a LED that indicates the current mode of operation. The LED is controlled by the Arduino. Figure 2-8 shows these connections conceptually.

The Arduino board, the multimeter and the tracking system are connected to the computer that runs the BoardLab software. The software was written in python 2.7 and runs on a PC with 4GB of RAM and a quad-core Intel processor running on Ubuntu 12.04. The software parses the design of the PCB and the associated schematic from Eagle 6.0 .brd and .sch files respectively. The board file (.brd) is parsed to create a layout map of all the features of the PCB. The position and orientation of the probe is used to compute the position of the tip. The position of the tip is then overlaid on the PCB map to identify the PCB feature to which the probe is pointing.

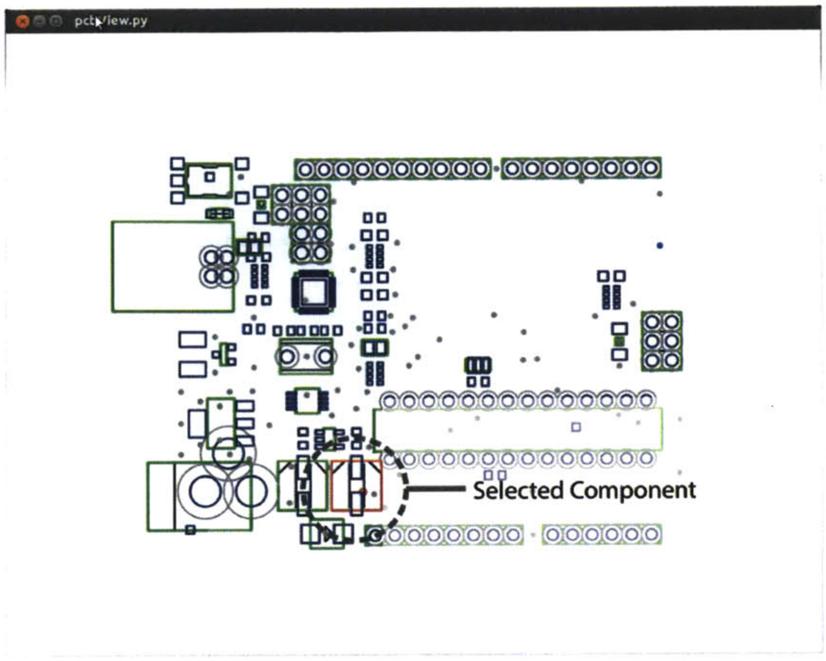

Figure 2-10: PCB symbol selected on the PCB feature map

2.4 Operation and interaction

The system is designed to work in the following modes: board positioning mode, component selection mode, voltage annotation mode and waveform verification mode. These modes are detailed below.

2.4.1 Board positioning mode

The tracking system tracks the position of the probe with respect to the work table, as the tracking system transmitter is mounted rigidly on the work table. The position and orientation of the probe need to be transformed to the coordinate system used on the circuit board. The board-positioning mode is a way for the user to tell the system where the circuit board is located on the work table.

In order to position the board, the user clicks the probe tip on three or more preselected via holes on the circuit board. The tip position and orientation data is then used to find the plane of the circuit board. Once the plane is determined, a least squares 2D point cloud match is applied to calculate the displacement of the origin and the angle by which it should be rotated in the plane. Section 2.3.2 describes how the data collected from board positioning mode is obtained. This process generally takes a user approximately 1-2 minutes to complete.

The probe tip vector is projected on the PCB plane to estimate where coordinates of the probe point on the PCB.

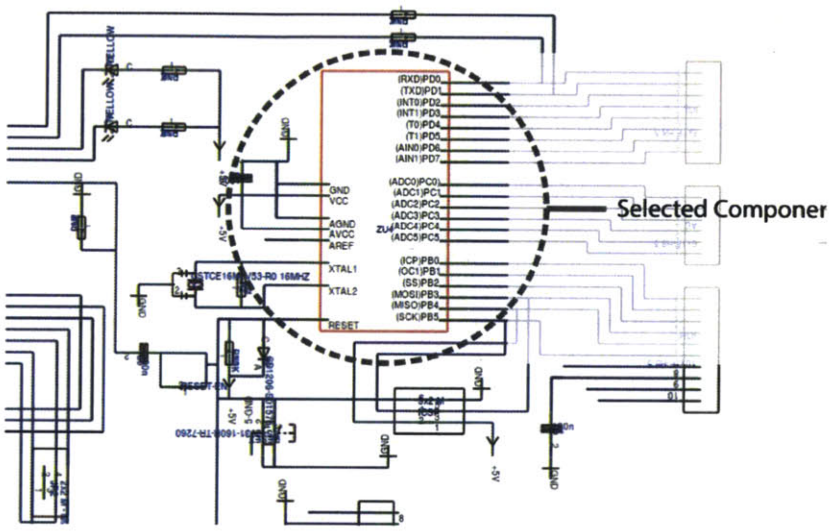

Figure 2-11: Schematic symbol selected on schematic display

2.4.2 Component selection Mode

In the component selection mode, the probe allows the user to select a single component. In this mode, the view highlights the selected component in the schematic. The motivation is to help the user understand how the component is connected with other components. If the component has a datasheet attribute, the view also loads the datasheet for the component.

2.4.3 Voltage annotation mode

Over the course of testing a PCB, a user might make many measurements of voltage across different nodes on the circuit. Conventionally, the user has had to manually understand what a measurement made on the PCB means in the context of the

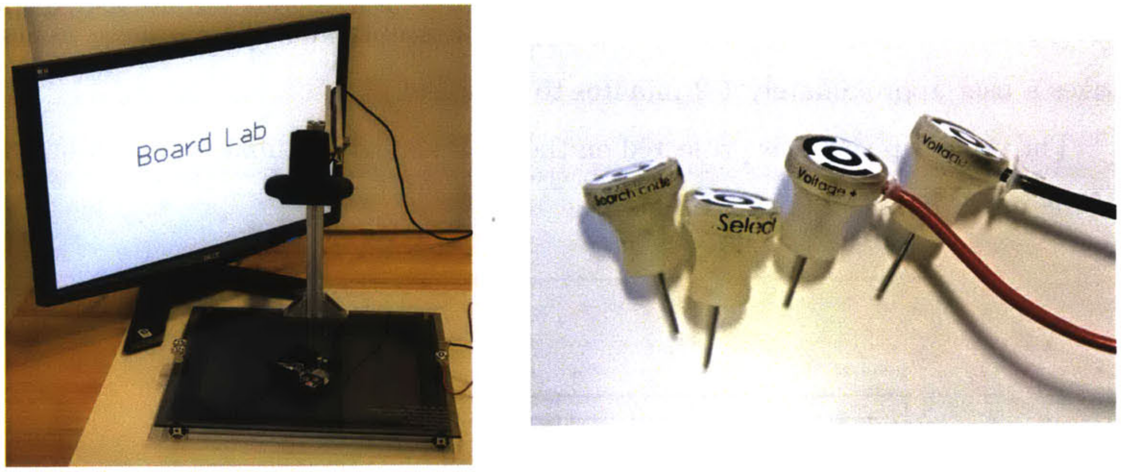

Figure 2-12: The first prototype of BoardLab using camera and AR fiducials to track the probes. Left: Complete system with camera and stand. Right: Probes with AR fiducials

schematic. The voltage annotation mode allows for automatic annotation of the schematic with the voltage measured using the probe, together, with the expected voltage when the board is operating properly.

2.4.4 Waveform verification mode

Oftentimes, circuit board design allows for simulating sections of the circuit board to generate expected waveforms. In the waveform verification mode, the expected waveform at the measurement point is plotted with a graph of real measurements.

2.5 Design history

The BoardLab project went through many design revisions, both on the level of the whole system and on the level of software and probe designs. In this section, I highlight some of the major revisions to shed some perspective on the design choices that led to the final version.

2.5.1 First prototype: Camera based tracking, KiCAD

The first prototype of BoardLab (Figure 2-12) used a 1920p webcam and visual fiducial markers for its tracking system. Visual tracking is unaffected by ferros or conductive proximate objects, but suffers from occlusion, etc. In this single-camera implementation, I resolved only 2D tracking co-ordinates, however, and soon realized that the 2D position estimation limitation of the system made it difficult to use. The software for the was designed to use Kicad EDA software files.

2.5.2 Second prototype: Magnetic tracking, Eagle

To overcome the limitations of the camera-based tracking system, it was replaced with a Polhemus Fastrak magnetic tracking system (Figure 2-16). This allowed the probe tip positions to be estimated much more accurately at a much higher framerate (120Hz). The tracking sensor is mounted away from the probe-tip, hence, removed from the conductive traces of the circuit board to minimize eddy-current distortions. This also led to the conception of BoardLab as a smarter oscilloscope probe and hence a smarter hand tool.

Probe design

The first design of the probe for this prototype (Figure 2-13) did not allow for any user input buttons on the probe. The next revision in probe design had two buttons mounted on a fin extending radially from the probe (Figure 2-14). This design turned out to be cumbersome to use in practice. The buttons are included more seamlessly in the current revision of the probe design (Figure 2-15): the main trigger button was located in the tip assembly and the secondary mode button was moved to the back end of the probe, drawing an analogy to the button on click pens. While this design was much more usable, it has a mechanical flaw: the probe tip assembly has a certain amount of play with respect to the main probe body to which the sensor is mounted. This reduces the positioning accuracy for the probe tip. Redesigning the probe to remove this flaw is one of the aspects of future work. Also, the torque

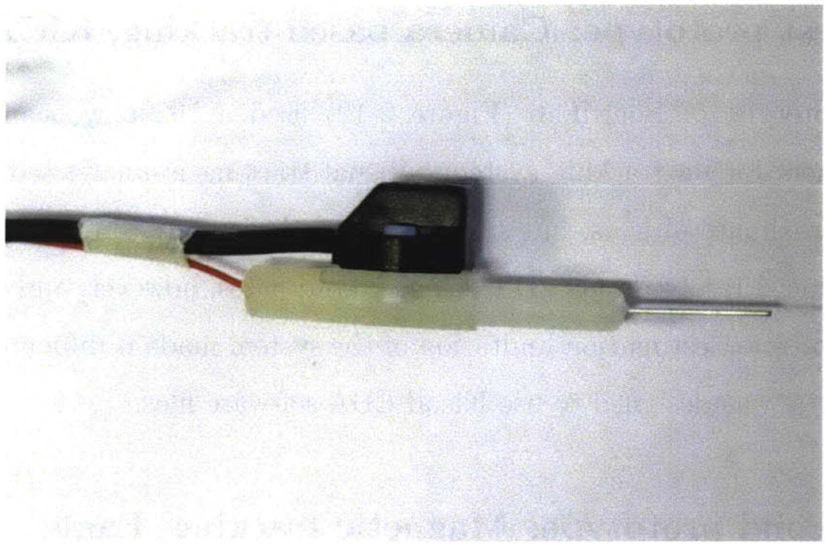
Figure 2-13: The first design of the probe.

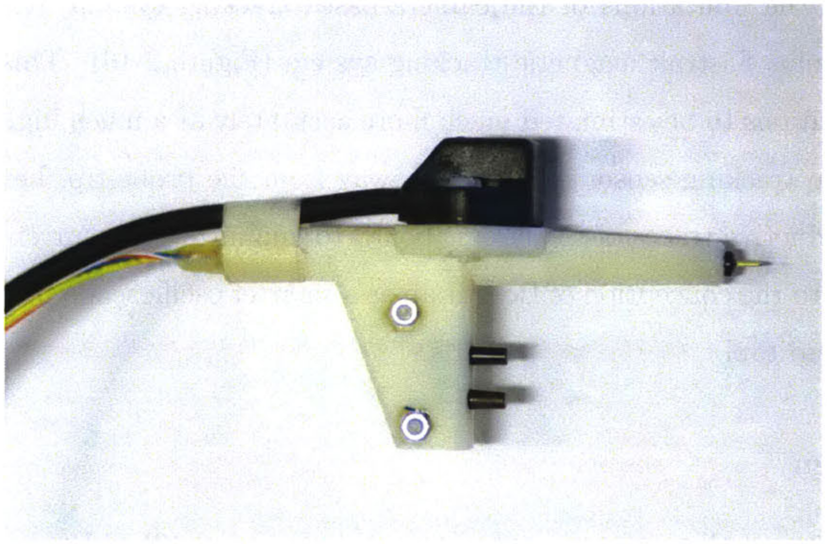
Figure 2-14: The first revision of the probe.

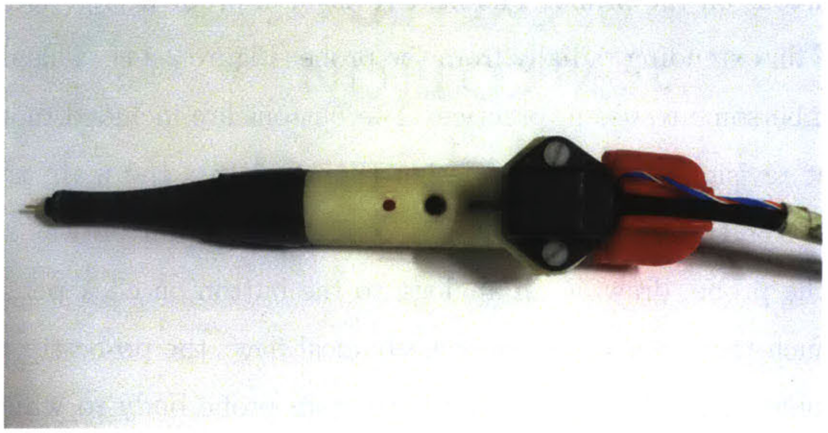
Figure 2-15: The current (second) revision of the probe.

Figure 2-16: Probe revisions for the second prototype of BoardLab using magnetic tracking system

applied by sensor wire was enough to tilt the sensor a tiny bit with respect to the probe. This was then fixed by creating a wire-holding fixture, resulting in a significant improvement in the accuracy of the probe tip position estimation.

Software design

In the second prototype, the PCB layout and schematic file support was moved from Kicad to Eagle 6.0. Some of the reasons for this change are:

1. Eagle 6.0 uses a XML based file format, which allows for extending the file with external data, including PCB positioning data, simulation verification data, etc.
2. XML based file structure allowed a custom Eagle 6.0 file parser to be written from scratch, which in turn allows for deep support of BoardLab actions.

2.6 Discussion and future work

The system was used with an Arduino Duemilanove board to test the system. This common circuit board matched with the design objectives that project was set out to solve in the initial design sketches; to be able to query and annotate the design data for a circuit using a probe to point to features on a real circuit board. The system allowed me to quickly build intuition about how different components are connected using the component select mode. This was useful for determining the functions and values of passive components: capacitors and resistors. The voltage annotation mode was useful in determinining the input voltage to the voltage regulator IC and in making sure that the part is functioning properly. Automatic annotation of voltages on the schematic worked in complement with my own reasoning of the circuit board, where, I tried to remember the node voltages for different nodes internally to make sure that the circuit board is functioning as expected. The handtool format of BoardLab allowed me to use the tool just like an oscilloscope/multimeter probe, thus building upon my previous understanding of using measurement probes.

A comprehensive user study would reveal more about what aspects of the design needs to be changed, and what aspects of the current system make it desirable to be used in electronic design and prototyping cycles. This being said, there are a number of technical aspects that I could not explore in the duration of the project that could be taken up as directions for future work.

Probe design

One of the basic mechanical requirements of the probe is to provide for a solid rigid mechanical connection between the probe tip and tracking sensor. However, in the last probe design the probe tip slides in a cylindrical cavity inside the main probe body. This construction, especially when done in plastic, allows for a large amount of angular play in the probe tip assembly with respect to the main probe body. I suggest that this could be changed so that the probe tip assembly be the same mechanical body as the sensor mount, and the part of the probe that is held by the fingers be constructed in such a way to slide on the probe assembly. Also, an RGB LED on the probe could be a better means to communicate to the user about the current system state.

Code highlight mode

Microcontrollers are quite commonly used in modern electronic circuits. Most microcontrollers are programmed in languages like Assembly, C, C++, etc. The code highlight mode would allow the user to introspect the code related to a node or a trace on the PCB by highlighting the lines of code that refer to the pin of the microcontroller connected to the node. This would make the probe a physical interface to query the firmware code for a circuit board.

Software design

The current system has its own rendering system to render the schematics and the PCB layout. This makes the software design too inflexible to adapt to different file structures used by different EDA software. The software could be redesigned to work as a plugin with the EDA software, allowing the rendering to be taken care of by the

EDA software. This also allows the user to keep using a software package with which they are already familiar to.

Chapter 3

Nishanchi

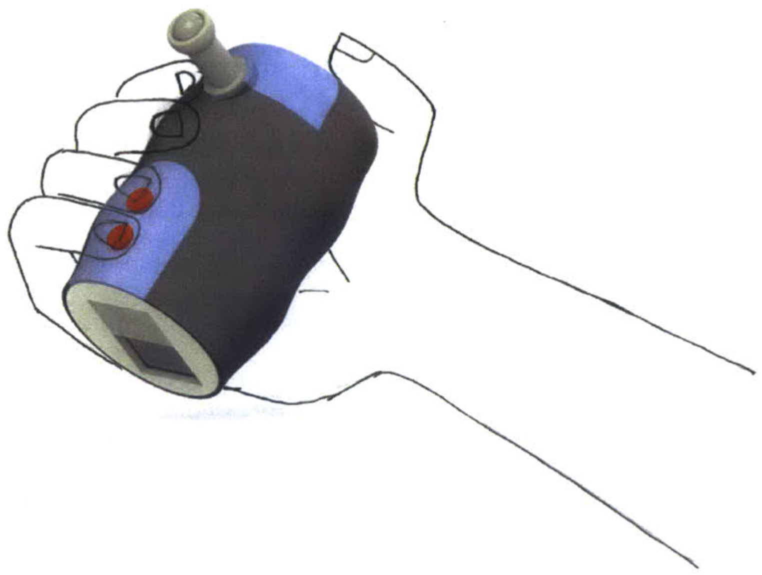

Figure 3-1: Nishanchi concept graphic. The similarity of the device with the shape and size of a typical hand-launched grenade is purely coincidental.

3.1 Introduction

Before the advent of NC (Numeric Control), the designs for objects were described on paper in the form of blueprints and sketches. Elements from these designs would then often be copied onto the workpiece for reference using pencils and/or stencils.

CAD (Computer Aided Design) now allows for creating detailed designs in the form of computer models. However, CAD does not work seamlessly in manual fabrication workflows. One of the problems is the sudden change of medium from the workpiece to the computer and vice versa, while importing features to the workpiece in the software and bringing design parameters back to the workpiece. Nishanchi is a position-orientation aware handheld inkjet printer that can be used to transfer the reference marks from CAD to the workpiece. Nishanchi also has a digitizing tip that can be used to input features about the workpiece in a computer model. By allowing for this two-way exchange of information between CAD and the workpiece, I believe that Nishanchi might help make inclusion of CAD in manual fabrication workflows more seamless.

3.1.1 Printing on non-conformable surfaces

While printing on simple curved and planar surfaces can be done using screen printing processes, printing on non-conformable, compound surfaces (for example aircraft tails) has to be done manually. While printing a general pattern on a compound curved surface could be achieved by a heat-transfer tape applied on the surface, it is difficult to maintain a good reference to the object's geometry when the objective is to apply the design consistently on multiple pieces. Further, heat-transfer tape starts to become practical economically only when used in large volumes. The Nishanchi printer could be used to print on such non-conformable and compound curved surfaces.

3.2 Printing CAD design parameters

In hand fabrication, most of the design parameters are marked on the workpiece by a pencil. Computer Aided Design can be used to create complicated models. In the absence of an effective method to transfer the design to the workpiece for manual operation, CAD data is reduced to diagrams for manual referencing. The Nishanchi printer can be used to transfer CAD design information onto the workpiece. Figure

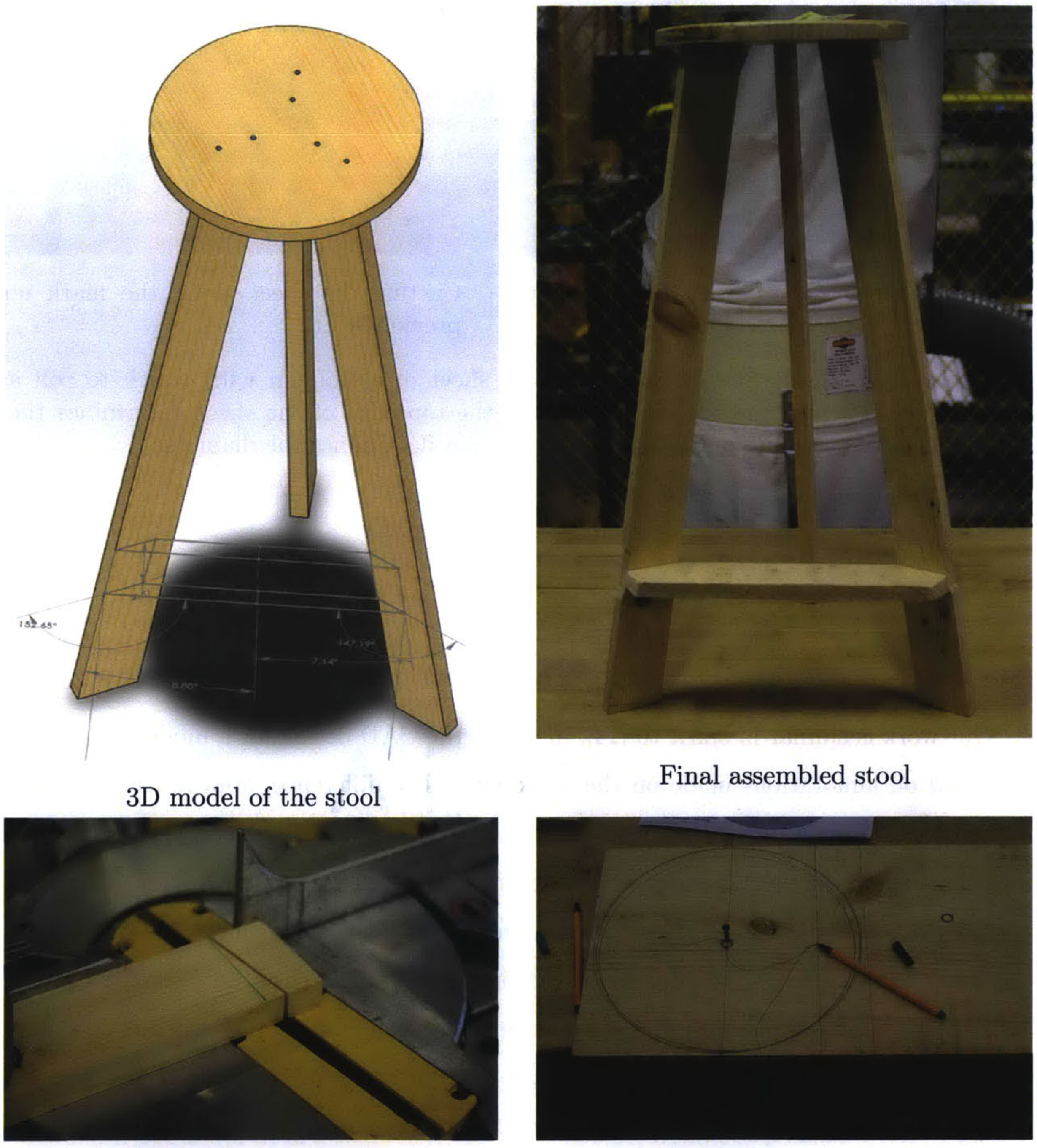

3D model of the stool

Final assembled stool

Marks on the stool legs

Marks for stool seat

Figure 3-2: Photographs showing how design parameters from the 3D CAD model of a stool are transferred manually to the workpiece.

3-3 shows a sheet metal worker making a mark on the sheet of the metal and then cutting along the mark made. Figure 3-2 shows how the design parameters from CAD

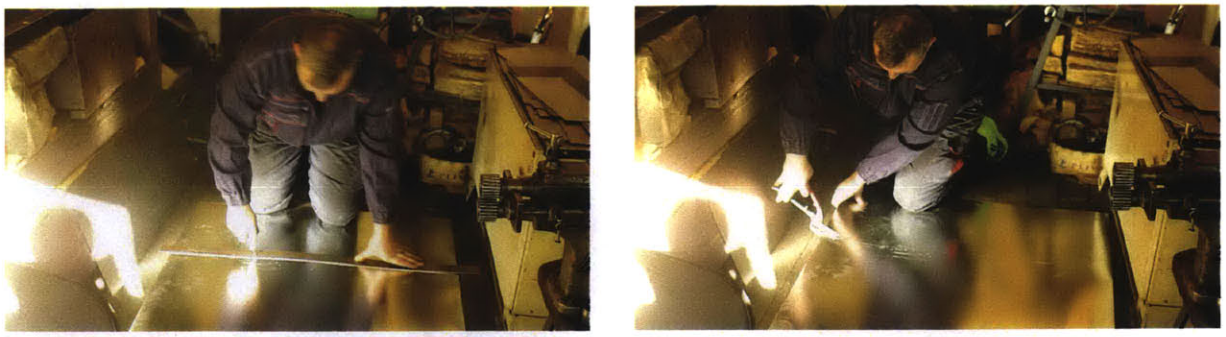

Marking the sheet for the height of the cylinder

Cutting the sheet along the mark made previously

Figure 3-3: Sheetmetal worker cutting a sheet of aluminum with which to roll a cylinder. The distance of the mark from the top edge of the sheet determines the height of the cylinder and length of the section determines the diameter.

software have to be marked on the workpiece manually.

3.3 Related work

Our work is similar in spirit to [14], in which the CAD design for a model is changed based on annotations made on the workpiece. The difference, however, is that Nishanchi also allows for transfer of the design back to the workpiece. Our approach is also similar to and is inspired by the approach used by [2] and [15], in which the handtool actuates automatically based on its position and orientation with respect to the workpiece. Although, my basic approach is similar to other handheld inkjet printers, for example [22], and the device usage is similar to [7] (in which the user moves the device back and forth to cover an area with a raster image), the key difference between Nishanchi and other handheld printers is that Nishanchi is aware of its 3D position and orientation, and it is aware of the 3D form of the workpiece.

3.4 Design and technology

Nishanchi is designed to be used like a paint roller. The user moves the Nishanchi handset on the workpiece back and forth to raster the desired area with a graphic

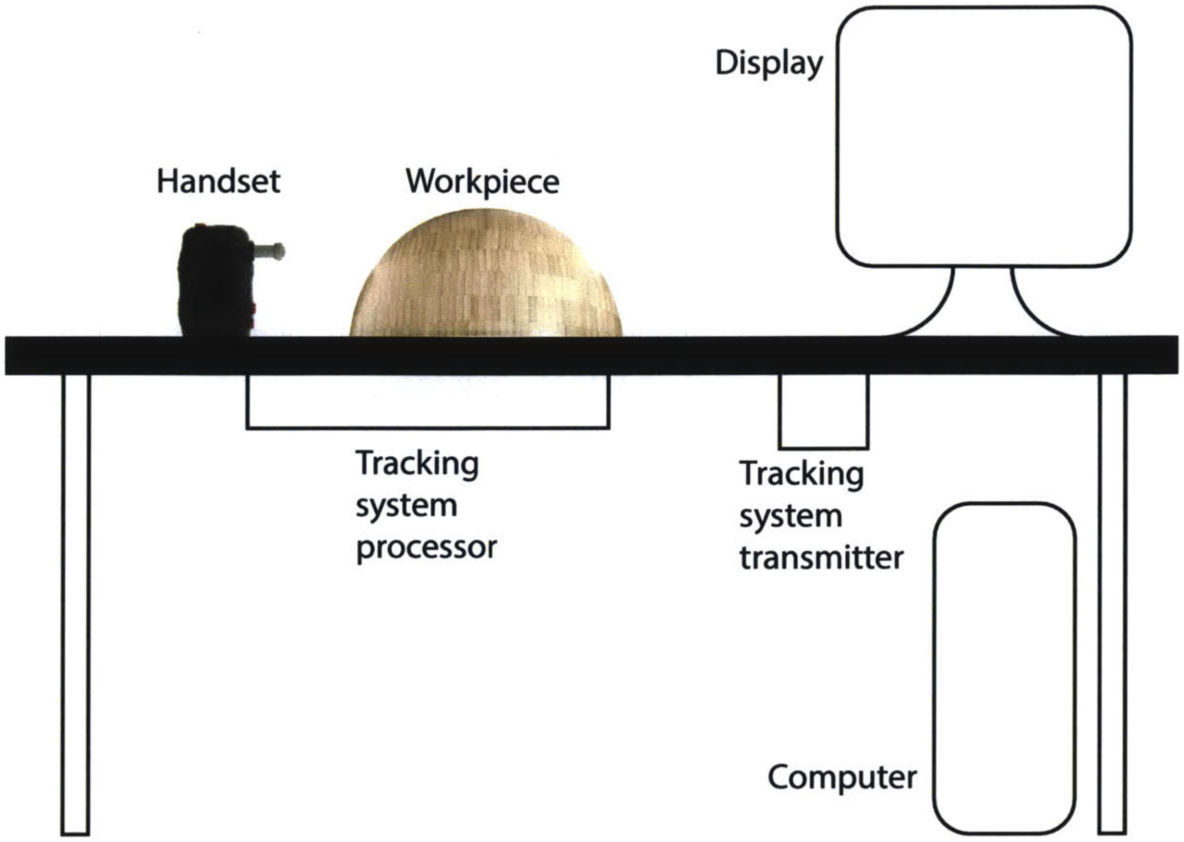

Figure 3-4: Nishanchi system overview

image. The handset is mounted with a MMTS (magnetic motion tracking system) sensor that works with a Polhemus FASTRAK system (an AC 6D magnetic tracking system) to estimate the 3D position and 3D orientation of the handset. Figure 3-4 shows an overview of the system.

3.4.1 Handset design

The handset device is made of 3D printed nylon. An inkjet printhead is mounted on the handset. The handset has two buttons mounted on the device that allow for the selection of digitizing vs printing mode. The buttons can also be used to activate special software functions.

As one of the important aspects of this work is to be able to print on non-conformable surfaces, it is important to have CAD models for the surfaces, and a way to register their physical position and orientation in the workspace with the

CAD reference frame. Further, oftentimes, it is not possible to acquire preexisting CAD models for all workpieces, so the Nishanchi handset is equipped with a digitizing tip to generate pointcloud data for the workpiece.

3.4.2 Inkjet printing system

Inkjet printing involves shooting droplets of ink by means of piezoelectric or thermoelectric actuation in nozzles mounted on a unit commonly called the inkjet print cartridge. One of the major advantages of this printing technology is that the ink droplets can be fired from a distance from the workpiece, allowing one to print without having to make mechanical contact with the workpiece.

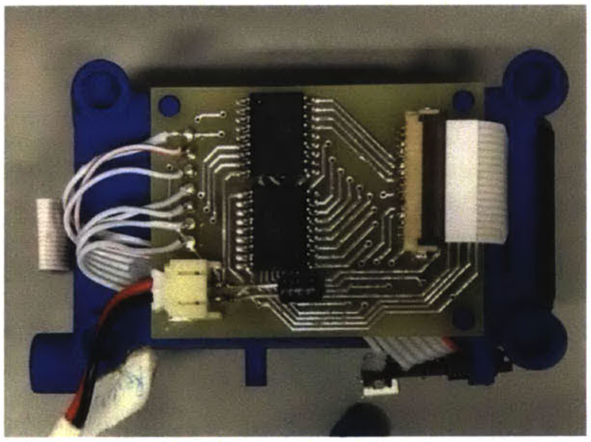

Figure 3-5: Photograph of the printhead control circuit board mounted on the handset

The print cartridges used on most commercially available printers use a proprietary control scheme. However, there is an open-source control board available for the HP C6602 inkjet cartridge [23]. The inkshield designs were used as reference to design and prototype a small electronic board (figure 3-5) suitable for the size of the handset, which could control a HP C6602 inkjet cartridge on the handset.

The HP C6602 inkjet cartridge consists of 12 nozzles arranged at a resolution of 96dpi. The cartridge exposes 13 terminals: the first 12 terminals are one each for each nozzle respectively, and the last terminal for ground. To shoot an inkjet drop from a nozzle, a voltage of 16v is pulsed once for a duration of about 20 milliseconds.

An ArduinoNano board drives the HP C6602 control board based on print data

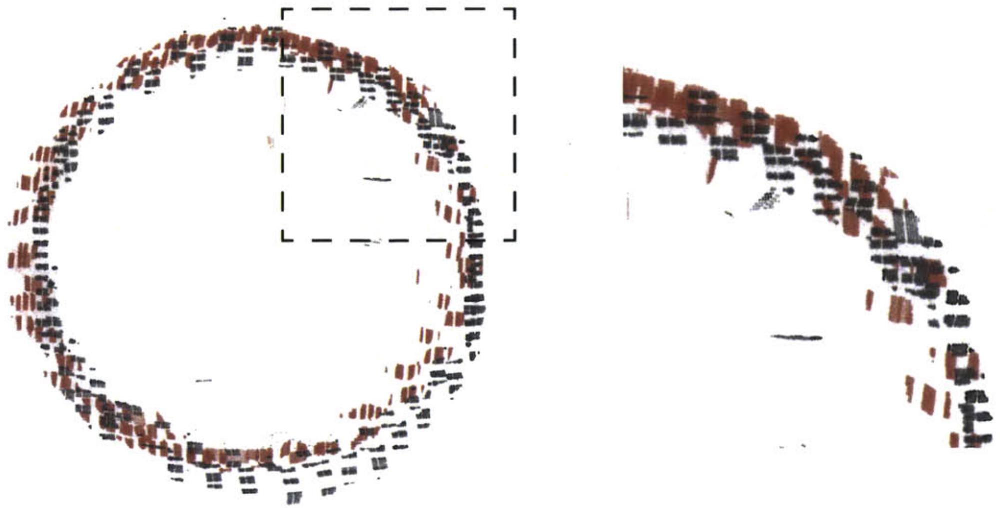

Figure 3-6: Scan of a print showing alternate white and dark bands because of the onboard FTDI buffers. Contrast this with figure 3-9 which was printed by tuning the USB FTDI buffers as described in section 3.4.2.

received from the computer over a Serial over USB connection. The FTDI chip used to handle the USB-Serial conversion has a receive buffer of 256-512 bytes depending on the exact part number. This buffering caused print frames from the computer to buffer in the receive buffer until the buffer reaches its limit; however, by the time this print frame data is sent to the Arduino over UART, the handset position has changed, causing inaccuracies in printing. The buffering also introduces banding artifacts (figure 3-6) in the printing. This happens because the arduino is starved of data while the FTDI buffer is still filling up.

This problem was fixed by setting the on-chip latency timers on the FTDI to 1ms ([24] and [25]), and by setting the event character to the last fixed byte of a print frame. This ensures that the FTDI chip flushes each print frame to the arduino as soon as it receives the end of a print frame.

3.4.3 Tracking system

The position and orientation state given by the tracking system is translated to get the position of the tip in the reference frame of the table. The Polhemus system can be configured to output the orientation data as a quaternion. Two frames of reference are used in the system: the ground frame of reference is fixed on the transmitter of the tracking system, while a second reference frame is fixed on the receiver. As the receiver is mounted rigidly on the handset chassis, this reference frame can be used to describe the positions of the digitizing tip and the inkjet nozzles on the handset. The CAD software plugin, however, uses the ground reference frame, as the workpiece is stationary and assumed to be fixed with respect to the transmitter.

3.4.4 Digitizing tip

The position of the digitizing tip is computed just like the probe tip for BoardLab as described in section 2.3.1. The tip offsets for the digitizing tip are found out in the same way they are found for the BoardLab probe tip as described in section 2.3.1.

3.4.5 Inkjet nozzle(s) position and orientation

In order to compute the position and orientation for each inkjet nozzle as the user moves the handset, the position of the nozzle with respect to the tracking system receiver needs to be determined. The tracking sensor was removed from the printhead to avoid interference and distortion on the tracker output. The digitizing tip for Nishanchi and the probe tip for BoardLab allow for an easy way of computing the tip offset vector (section 2.3.1). However, such a process for the nozzle offset vector would require a mechanical jig to hold the handset. In the absence of a jig, the calibration can be done in a two-step process as described in the following sections.

Coarse calibration

In the coarse calibration, the offsets were partly computed from the CAD model of the handset (figure 3-7) and partly computed using a high-resolution photograph of

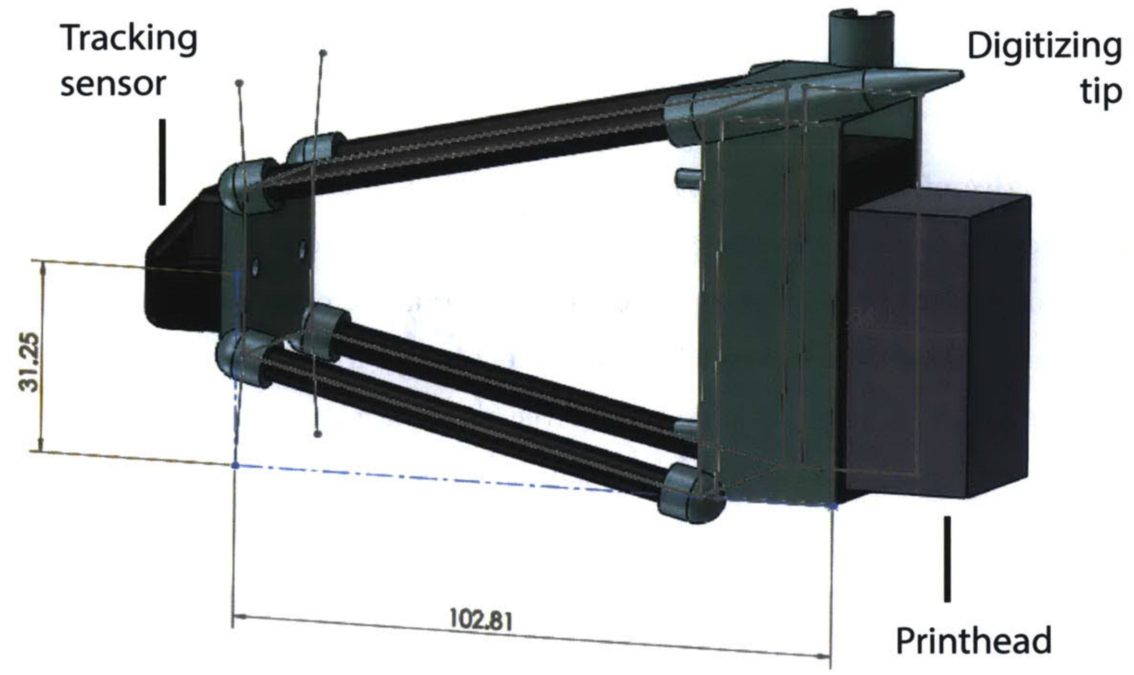

Figure 3-7: CAD model of the final prototype showing X and Z components for nozzle offset vector

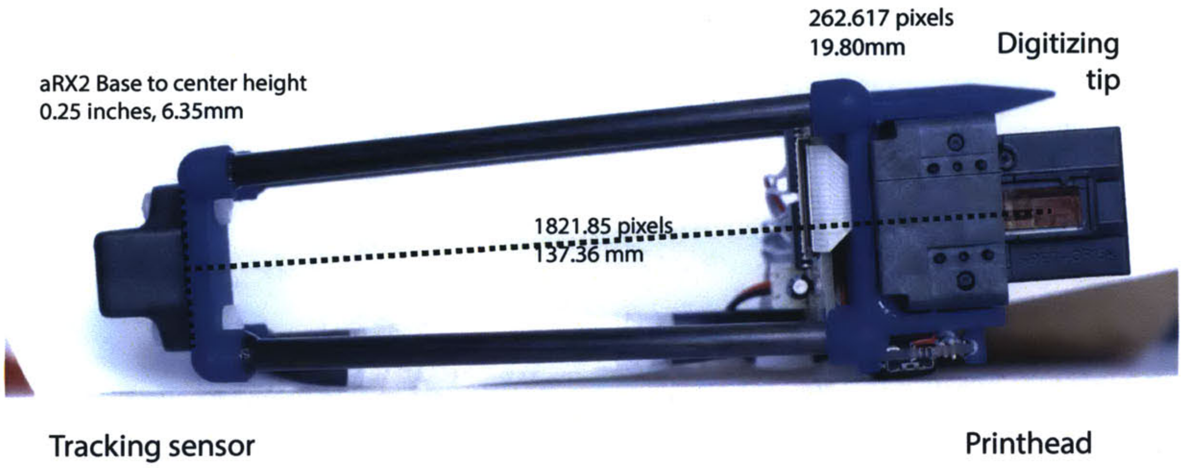

Figure 3-8: Photograph of the final prototype showing Z component measurement for nozzle offset vector

Coarse calibration

the model (figure 3-8). The objective of coarse calibration is to bootstrap the system to work so as to allow for collection of data for a finer calibration. Figure 3-9 shows remaining error in nozzle offset vector after performing only coarse calibration.

Fine calibration

The objective of fine calibration is to finetune the X,Y components of the nozzle offset vector. However, as the components cannot be directly measured, the fine calibration procedure is designed to isolate the error in the offset vector along the X and Y components. The technique relies on the fact that if the handset is used while being kept parallel to either of the axes, the resulting printed image is displaced by the error in the nozzle unit vectors along the axis. However, due to a lack of an absolute reference frame on the paper, this displacement cannot be measured directly. Printing another image using the handset in the exact opposite orientation (by rotating 180 degrees) produces another displaced image. The total displacement between the images is twice the offset correction that needs to be applied. To collect

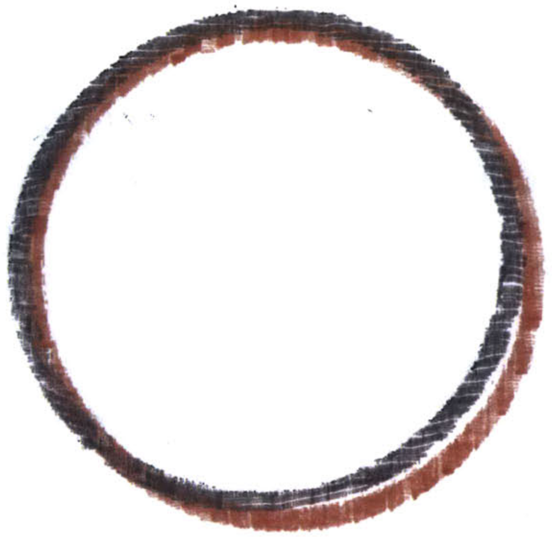

Figure 3-9: The Red and Black circles in this printout were printed by translating the handset in generally one orientation throughout the printing process for each circle, respectively. The handset was rotated by 90 degrees in the plane of the printout between the two colors. The displacement between the two circles shows the error in the nozzle vector values.

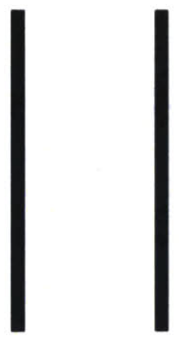
Figure 3-10: Two-lines calibration print

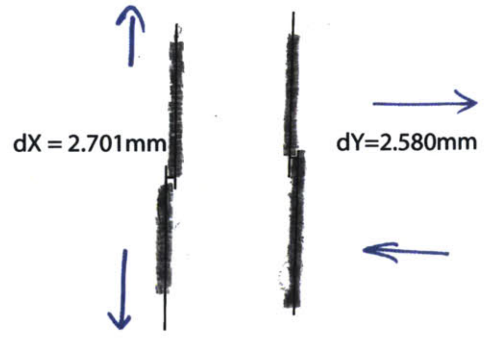

Figure 3-11: Calibration print showing broken displaced lines when connected parts of the lines are drawn keeping the handset in the orientation as shown by the blue arrows.

the calibration data, the system is used to print the two parallel lines as shown in figure 3-10.

The line on the left (figures 3-10 and 3-11) is printed while keeping the handset parallel to the line. The top part of the line is printed with the handset pointing upwards and the bottom line is printed with the handset pointing downwards. The resulting line segments are displaced by twice the error in the X component of the nozzle vector.

The line on right (figures 3-10 and 3-11) is printed while keeping the handset perpendicular to the line. The top and bottom parts of the line are printed with the handset pointing in the left and right directions, respectively. The resulting line segments are displaced by twice the error in the Y component of the nozzle vector.

The calibration print is then scanned and the displacement between broken line segments is estimated to compute the X and Y components of the correction. Figure 3-12 shows the drastic improvement after applying the corrections as calculated in the manner described above.

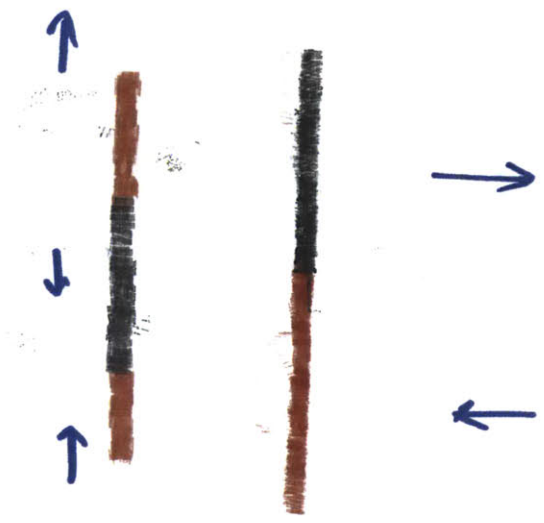

Figure 3-12: Post calibration print. Left: Printing across the line direction. Right: Printing across the line direction. The Red and Black sections differ in handset orientation by 180 degrees as shown by blue arrows.

Inkjet nozzle position and orientation

Once the nozzle offset vectors are known for each nozzle, the position and orientation for the inkjet nozzles in the reference frame of the transmitter are computed the same way that the probe and digitizer tip positions are computed in the manner as described in Section 2.3.1.

3.5 Software

The handset device is designed to work with a plugin written for the Rhinocerous 5.0 software. The software was chosen for its ease of use and solid plugin support. While planar graphics can be represented in a two-dimensional array of pixels, the representation on curved surfaces becomes non-trivial. I found that representing the surface as a mesh results in good nozzle trajectory surface intersection computation performance. At the same time, it is well supported by Rhinoceros. A limitation of this representation versus a mapped bitmap representation is that a mesh only allows for a monochrome representation of the shape.

When in printing mode, the software plugin computes the trajectories of all the nozzles on the printhead for each position frame reported by the tracking system. The software plugin, when in printing mode, computes the trajectories of all the nozzles on the print head for each position frame reported by the tracking system,. When the intersection distance for a nozzle trajectory is within a certain threshold the computer sends commands to the printhead to trigger the nozzle.

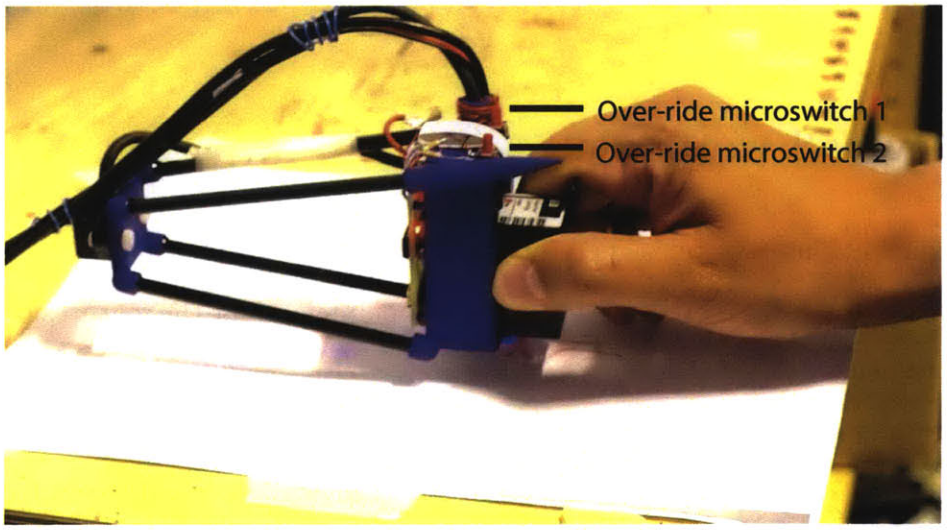

Figure 3-13: A photograph of a user using Nishanchi (final prototype) to make a print on paper.

3.6 Operation and interaction

3.7 Digitizing mode

The digitizing mode lets the user scan pointcloud data using the handset's digitizing tip. The spirit of including a digitizing tip in the device is to allow the user to use the same device as a means to import features of the object into the computer representation of the object. The user activates the digitizing tip mode by pressing the digitizing button.

3.8 Print mode

The print mode allows the user onto print a selected surface object in Rhinocerous on the object. This mode is activated by pressing the print button. There are two microswitches on the handset (figure 3-13). The microswitches can be used to override the computer control of the inkjet printhead as the device is used. The first microswitch overrides the computer to fire all the nozzles irrespective of whether the computer pattern requires ink at the nozzle position or not. The second microswitch overrides the computer to not fire any nozzle.

3.9 Overall workflow

The Nishanchi printer was designed for the following workflow:

1. The user uses the digitizing tip to create a pointcloud for the features of interest of the workpiece.

2. The pointcloud data is used to generate a CAD or partial CAD model using the point cloud data. As the point cloud data is referred to the transmitter of the tracking system, the CAD model of the object is in proper registration with the reference system.

3. CAD operations are performed on the computer model.

4. The results of the CAD operations are transferred to the object using print mode.

3.10 Design history

The Nishanchi project went through many design revisions, both on the level of the whole system, and on the level of design of the software and and the handset. Some major design revisions and the reasoning behind the revisions are shared in the following sections.

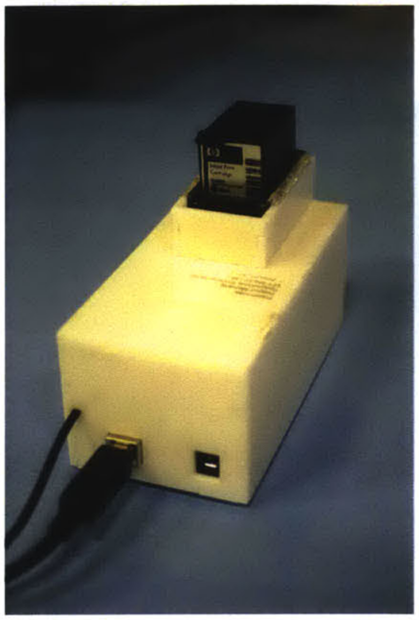

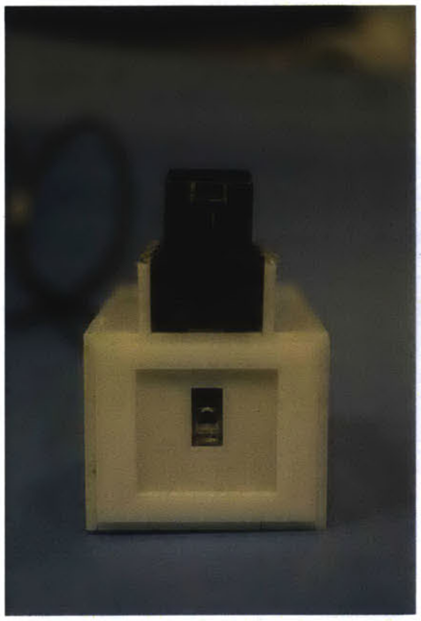

(a) Bottom view showing the optical flow sensor and inkjet nozzles

Figure 3-14: Nishanchi first prototype

3.10.1 First prototype

The first prototype of Nishanchi (figure 3-14) used an InkShield board housed inside an acrylic enclosure, mounted with an optical flow sensor appropriated from a Microsoft Comfort USB mouse. The flow sensor was used to track the position of the printhead with respect to the surface. Needless to say, I discovered that the integration of displacement values given by the flow sensor led to large drifts in the position estimate. Also, the optical flow sensor does not measure angular movements of the printer. In order to print successfully, a drift-free estimate of position was needed.

Figure 3-15 shows a screenshot of the python program that was written to print 2D raster images.

3.10.2 Second prototype

To make the second prototype, the Polhemus Fastrak sensor was mounted on the acrylic enclosure used for the second prototype. Also, a blue cardboard inlay was added to enhance the visual aesthetic of the handset (figure 3-16).

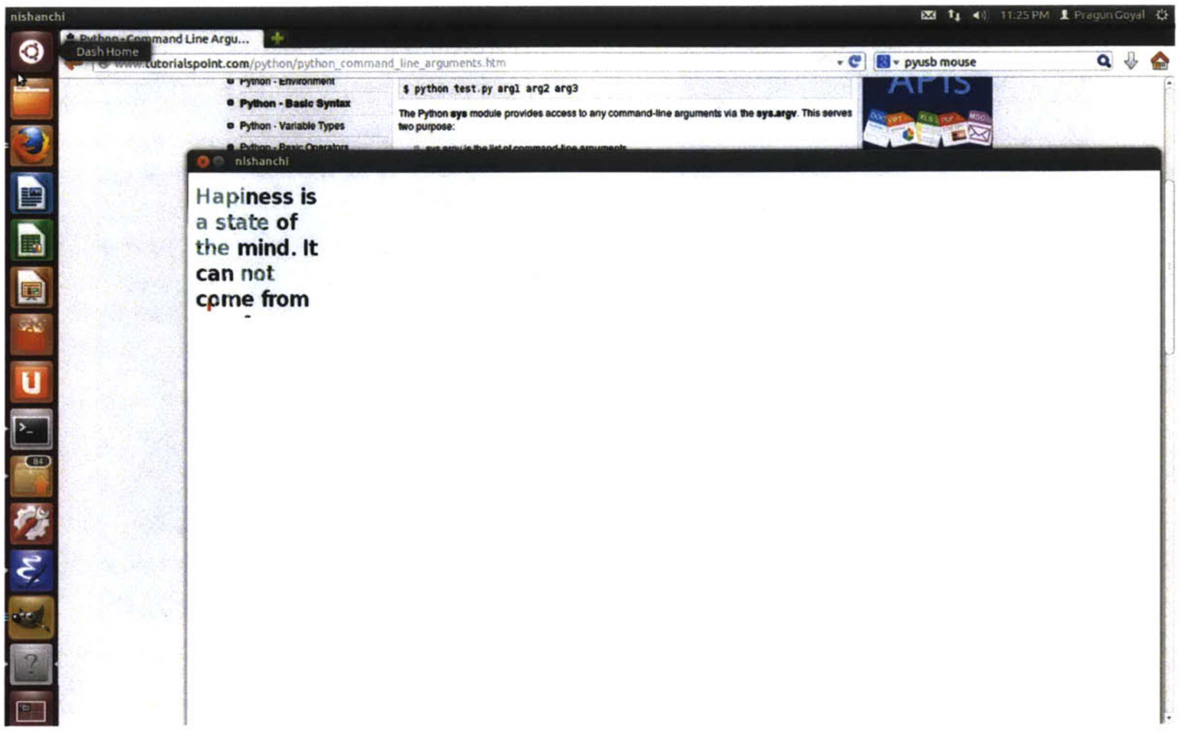

```
$ python test.py arg1 arg2 arg3
```

The Python sys module provides access to any command-line arguments via the sys.argv. This serves two purpose:

Hapiness is
a state of
the mind. It
can not
come from

Figure 3-15: The software for Nishanchi first and second prototypes. Cyan colored pixels have already been printed and the black pixels are yet to be printed. The red vertical cursor is the estimated position of the inkjet nozzles with respect to the image.

As this prototype was tested, I found that the tracking system performance would degrade drastically in the close vicinity of the Inkshield board. Upon more testing, I found that this was caused in part due to interference caused by the electromagnetic field produced by an inductor on the Inkshield board. This problem was temporarily solved by opening the acrylic enclosure and moving the inkshield board farther from the sensor. However, this established the need for a redesigned printhead control board that does not cause interference. Figure 3-17 shows one of the early printouts taken using the second prototype.

3.10.3 Third prototype

The handset (figure 3-19) for the third prototype was designed in Solidworks and 3D-printed in nylon. This allowed for introducing features like the digitizing tip and user control buttons in a more ergonomic form. Figures 3-20 show the different revisions

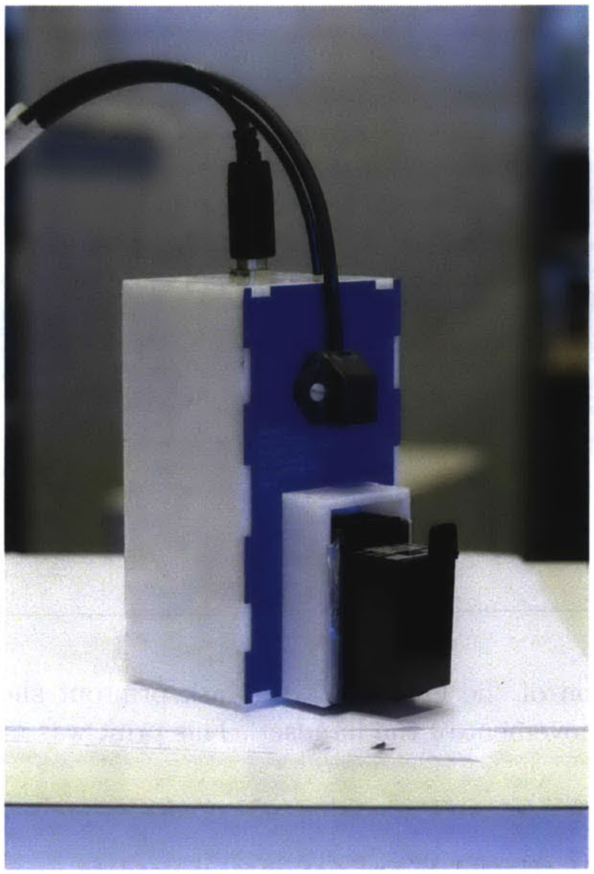

Figure 3-16: The second prototype. Notice the magnetic tracking sensor and the blue overlay.

of CAD models before finalizing the one shown in figure 3-18.

The bulky size of the handset made it difficult to guess where the printhead nozzles were located on the large base, and made it difficult to use the tool intuitively.

Software

The software for the third version was written as a Rhinoceros 5.0 plugin. Several different approaches were tried to represent the graphics in 3D. In the first approach, the graphics were represented as Rhino native NURBS objects. While this approach allowed maximum operatability with Rhino, experiments revealed that, for complicated surfaces, the computation time of finding the intersection of the nozzle trajectories with the surface was too large to be done in realtime for each frame.

In the second approach, I tried mapping the curved graphic to a 2D bitmap

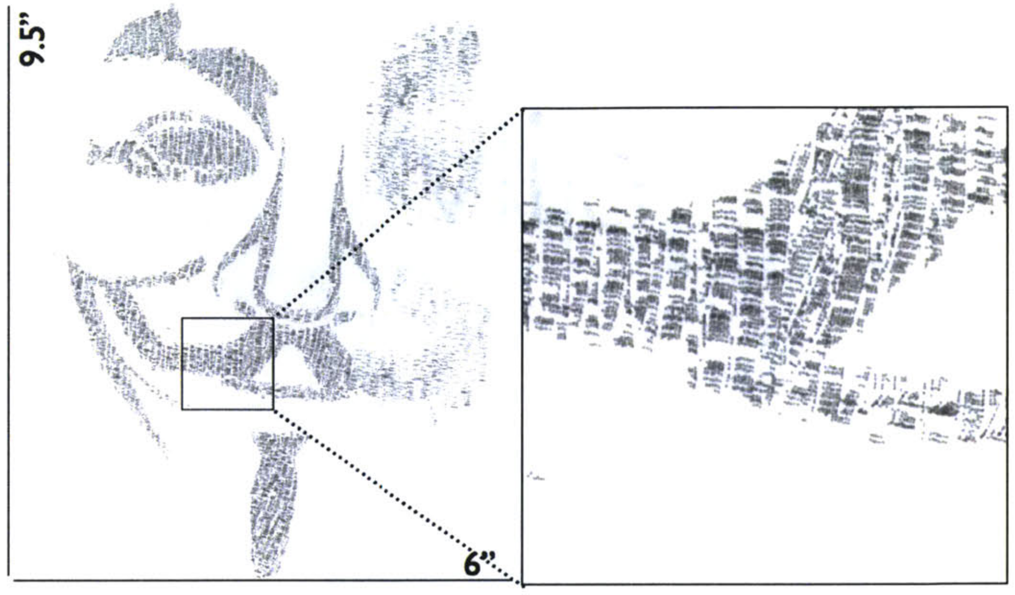

Figure 3-17: A section of the Guy Fawkes' Mask printout showing artifacts introduced by the user's movement of the handset. This print was made using the second prototype.

representation via UV (U and V are parameters used to map a curved surface to a flat X,Y surface) coordinate mapping. However, the Rhino software development kit does not support the generation of textures based on surfaces. Writing a UV coordinate mapping layer for Rhino turned out to be out of scope for this thesis.

The approach that I finally selected was representing the 3D graphic as a mesh object. This allowed for an efficient computation of nozzle ray intersections while being within the API support of the Rhino plugin development toolkit.

Electromagnetic interference

The third prototype featured the smaller printhead control circuit board (figure 3-5), which removed onboard switched-mode DC-DC voltage conversion, which in turn removed the electromagnetic interference caused by the switching. However, the current spikes associated with firing inkjet nozzles still produced enough magnetic field to interfere with the tracking system each time a nozzle is fired. The handset needed to be redesigned with the magnetic sensor moved farther away from the printing

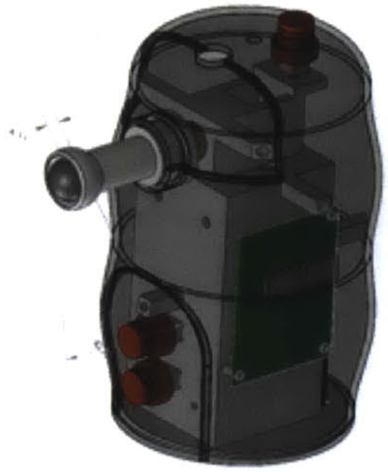
Figure 3-18: The solidworks CAD model of the handset showing internal chassis that mounts the circuit boards, buttons, tracking sensor, digitizer and printhead.

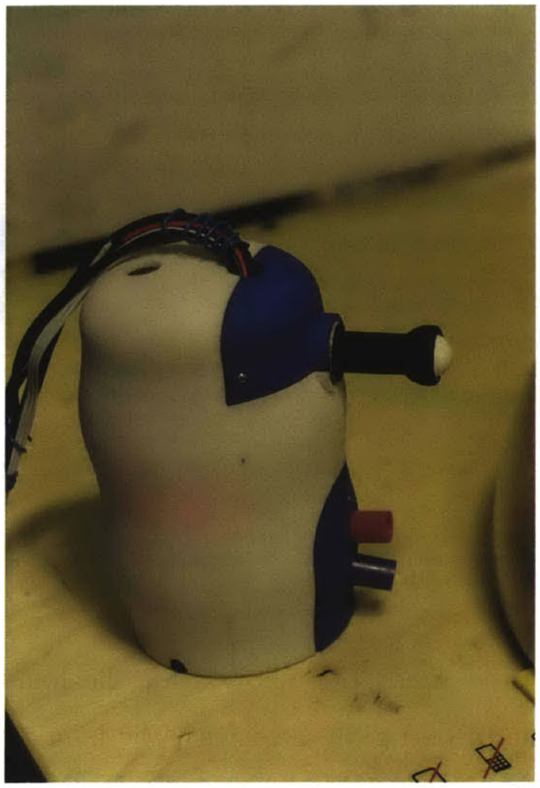
Figure 3-19: 3D printed third prototype

assembly to solve this problem completely. In order to test the prototype, the printing rate was decreased to about 5-6Hz; this provided the filters in the tracking system enough time and measurements to reach an accurate estimate of sensor position and orientation before the nozzles are fired again. This results in a very slow print rate.

3.10.4 Fourth prototype

A fourth prototype was built to overcome the issues in the third prototype. Some of the design requirements for this prototype were: moving the sensor farther away from the printing assembly, reducing base area so that the user can clearly see the printhead, and reducing the size so that the handset does not obstruct the view to the workpiece. Figure 3-7 shows the Solidworks CAD model for the prototype, and figure 3-8 shows the final assembled prototype. Carbon fiber tubes were used to create a platform for the sensor away from the printing assembly. Carbon fiber is extremely

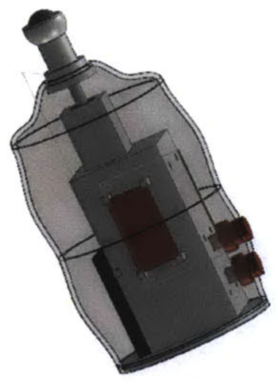
Figure 3-20

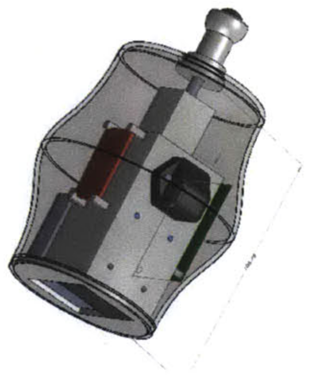
Figure 3-21

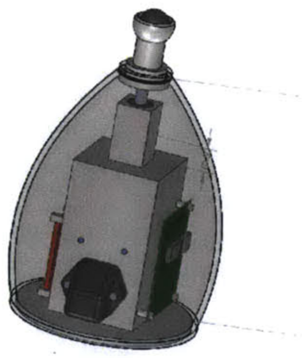
Figure 3-22

Figure 3-23: CAD models of different handset designs before the third prototype, shown in figure 3-19

light and rigid; this allowed for the handset to be lightweight, while allowing the sensor to be rigidly held with the handset. The sensor was positioned about 12cm away from the inkjet printhead control electronics. This reduced the electromagnetic interference caused by printing, and allowed for a print-rate of about 40Hz. The nozzle offset vector for this prototype was calculated using the coarse-fine calibration procedure described in sections 3.4.5 and 3.2.

3.10.5 Printing in 2D: Guy Fawkes mask

While Nishanchi was designed to print on 3D non-conformable surfaces, during preliminary testing I found that using the tool in 3D takes some practice and acclimitation. So, the first user study involved printing on 2D surfaces to understand how users use the tool to make prints without introducing the complexity of printing in 3D.

Six users were asked to make a print of a monochrome image of the Guy Fawkes Mask (figure 3-24). The users were given red and black ink cartridges to make the print. The print size was about 15cm x 20cm. The users were asked to describe their impressions of the tool and the issues they faced while they used the tool. The toolpath, printhead command and override button data were logged as the users created their prints.

Figure 3-24: The original image used for Guy Fawkes mask.

3.10.6 Quantitative analysis

The overall framework for analysis of usage data was adopted from Zoran et al. in [26]; however, the features for the analysis were chosen to be relevant to the use of the device while making a print. Position, orientation, printhead control, and override button data were collected for each user. Printhead velocity was obtained by applying the Savitzky-Golay gradient filter on the position data. Speed and direction of the projection of velocity on the print surface were calculated from the velocity estimate. Orientation data was used to compute a unit vector collinear with the nozzles (Swath unit vector). The angle between the swath unit vector and the velocity vector indicates if the the user moved the printhead along the swath or across it. The height of the print head above the print surface was computed from the position and orientation data. These features were clustered using Gaussian Mixture Models or K-Means clustering algorithms. The resulting labeled data was consolidated into 60 second segments by a simple per-label datapoint counting scheme. The resulting label counts were weighted linearly by the fraction of total print frames that were sent to the printhead in the segment. Figure 3-25 shows an overview of the quantitative

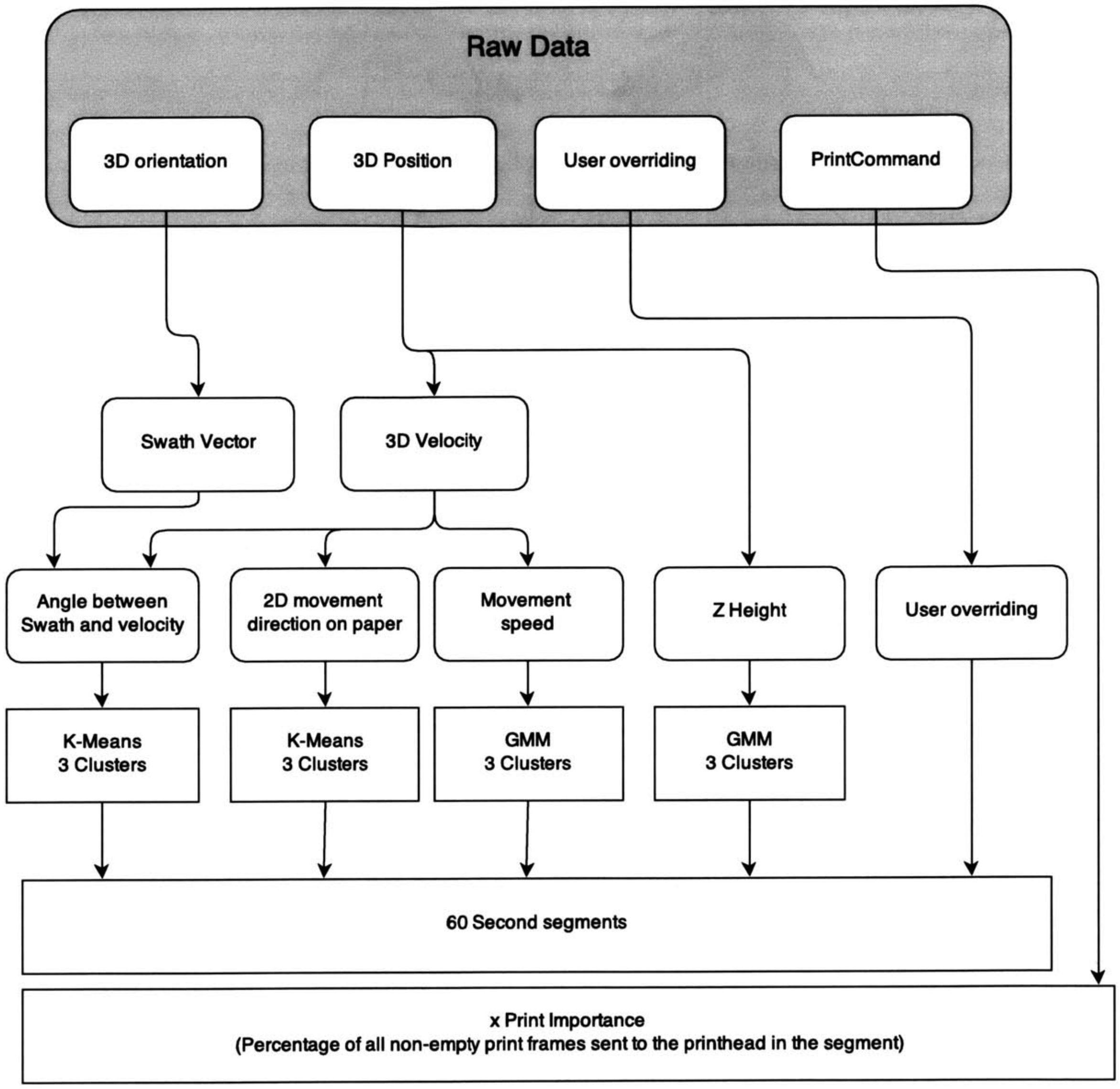

Figure 3-25: Userdata features and clustering

analysis. The resulting data is plotted in figure 3-26, and provides insight on how the users used the device while making the print.

Description visualization and usage data figures

The top right subfigure in figures 3-27, 3-28, 3-29, 3-30, 3-31 and 3-32 shows the 2D projected toolpath used by user to make the print shown on the top left subfigure. Each dot represents a recorded handset position. Red dots represent the positions where the computer automatically controlled the nozzles. Black dots represent posi-

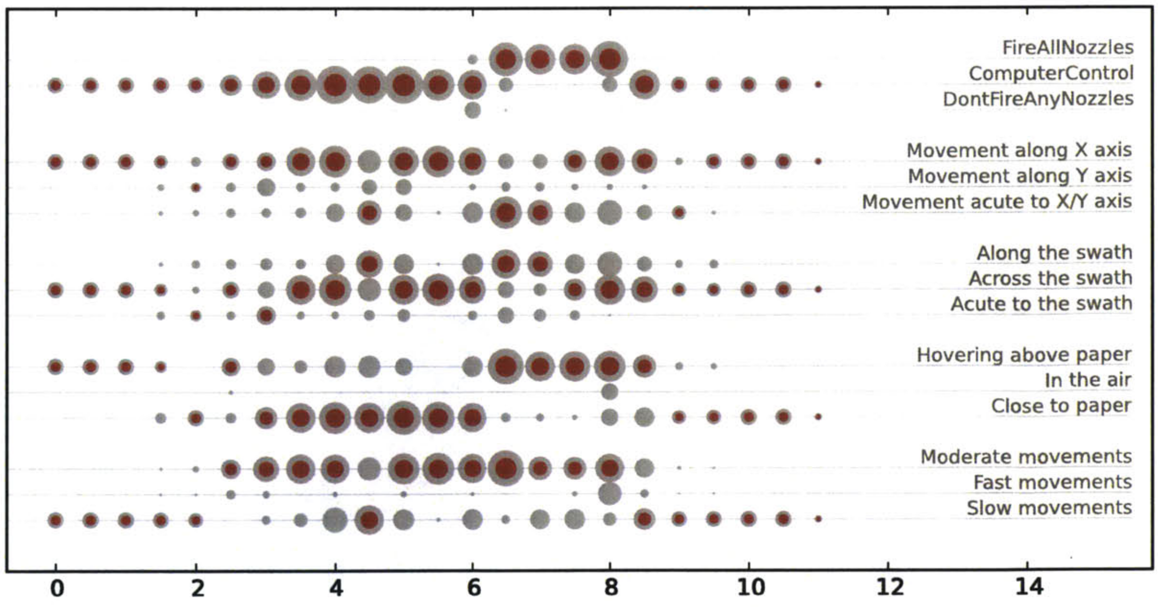

Figure 3-26: Plot showing the analyzed tool usage data for user Santiago. Section 3.10.6 describes this figure in detail.

tions where the user overrode the computer to fire all nozzles. Magenta dots represent positions where the user overrode the computer to not fire any nozzles. Cyan dots represent all other positions where the tool was recorded at but where no nozzles were controlled.

The bottom plot shows different facets of techniques used by user to make the print shown in the top left subfigure. Each circle represents 60 seconds of use. The size of a circle represents the time and importance of a facet in a 60 second segment. Red circles represent the most used facet in a segment.

3.10.7 User impressions

Alexis

Alexis is a graphic artist and she paints with oil and watercolor. This can be seen in her print (figure 3-28) as well. She used the tool slowly with repeated back and forth motions to create thick, dark, paint brush-stroke like textures. Of all the users, Alexis was the only user who used black and red ink extensively. Alexis also used a white correction tape to cover sections she accidentally printed over. This led to

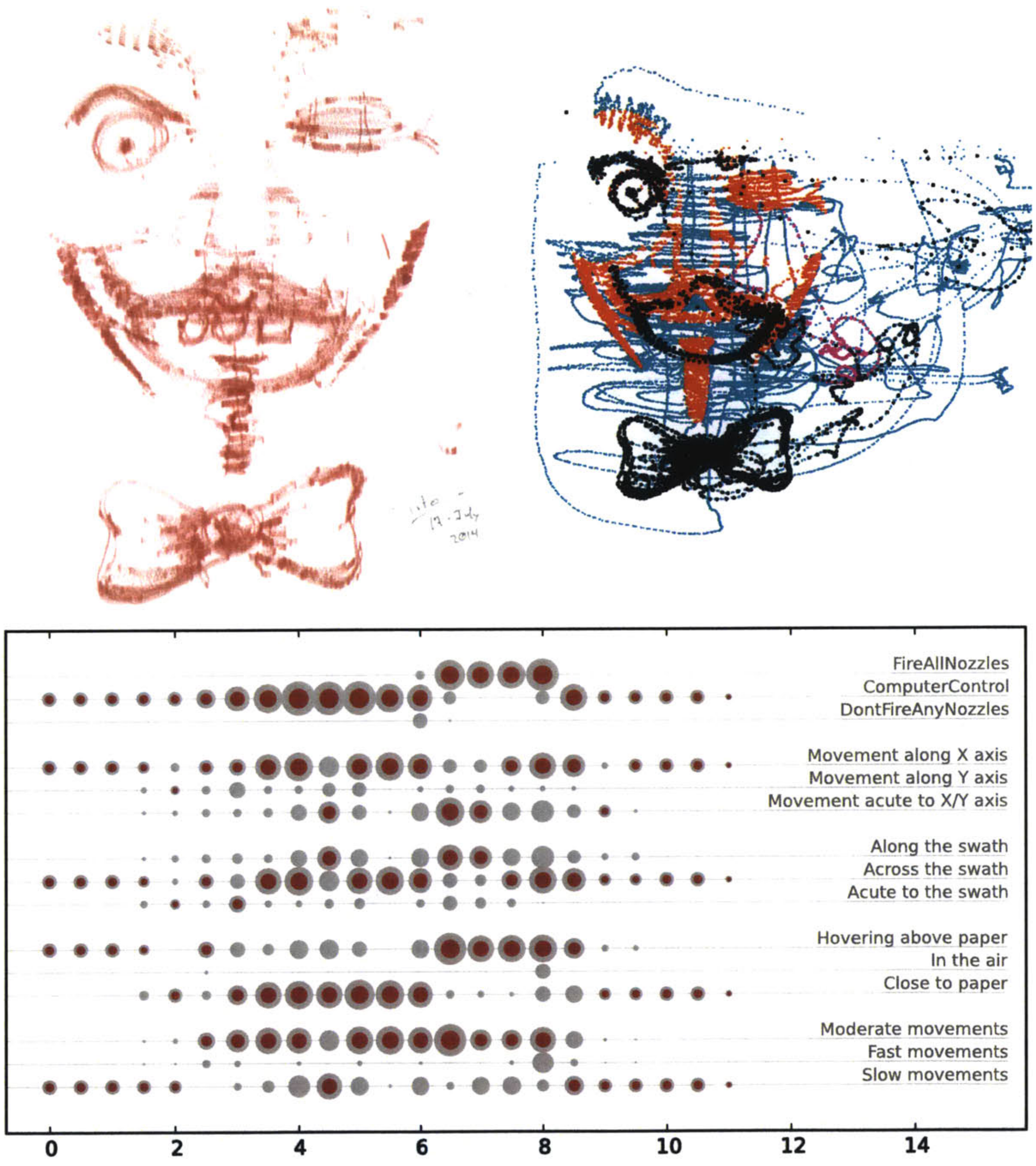

Figure 3-27: Top left: Santiago's print. Top right: Visualization of handset position data. Bottom: Visualization of usage data.

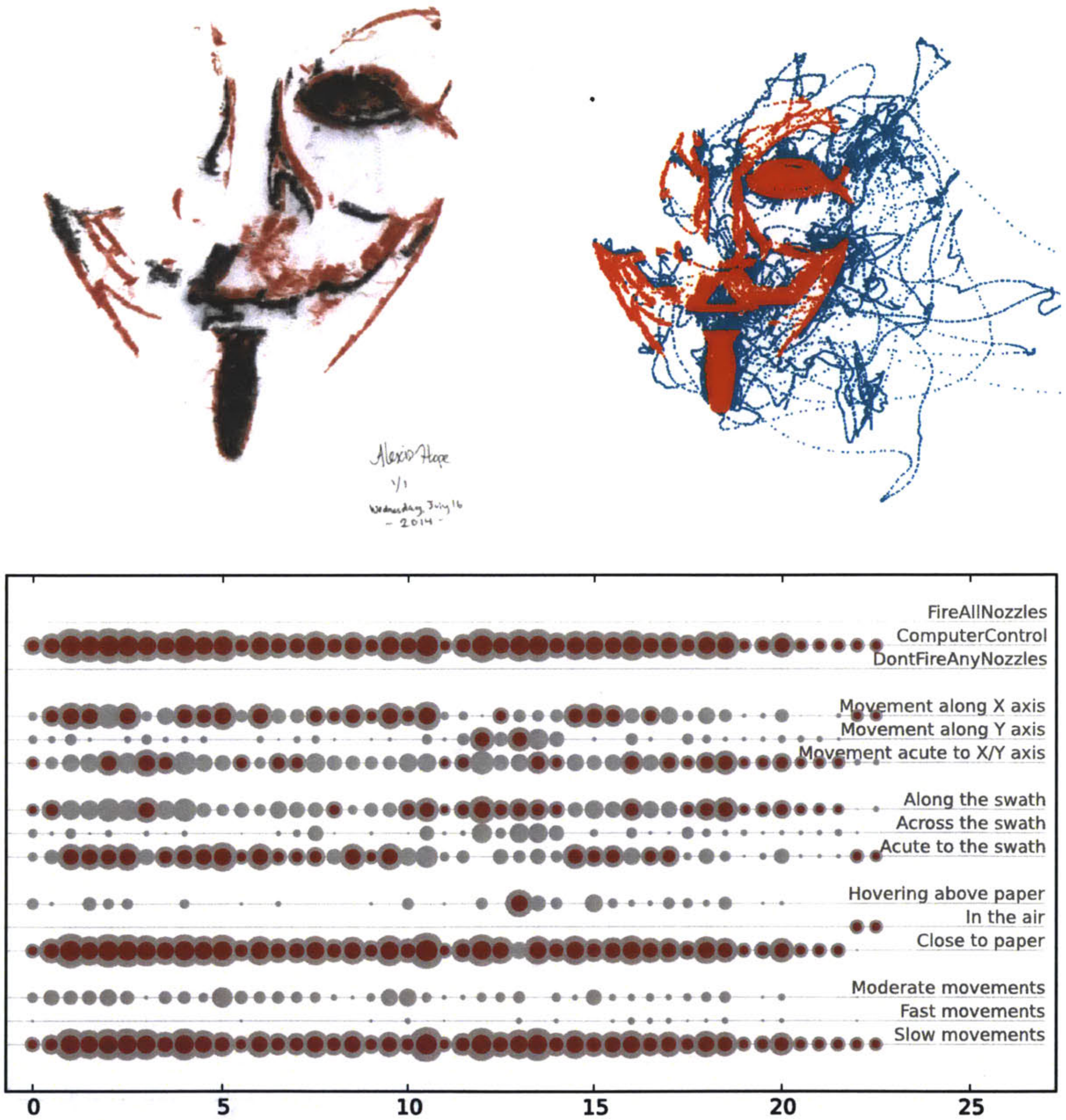

Figure 3-28: Top left: Alexis's print. Top right: Visualization of handset position data. Bottom: Visualization of usage data.

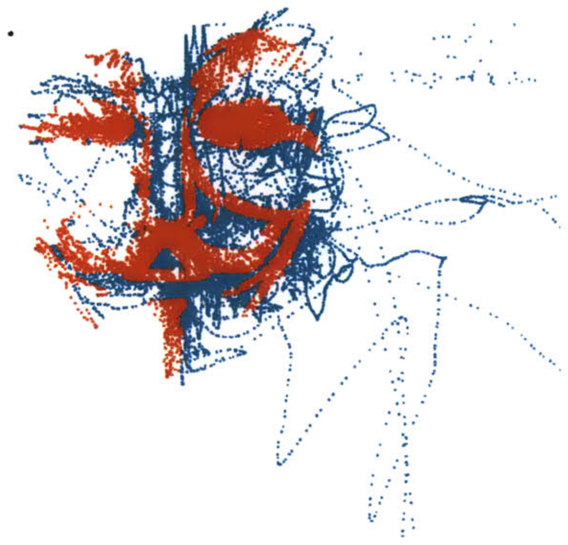

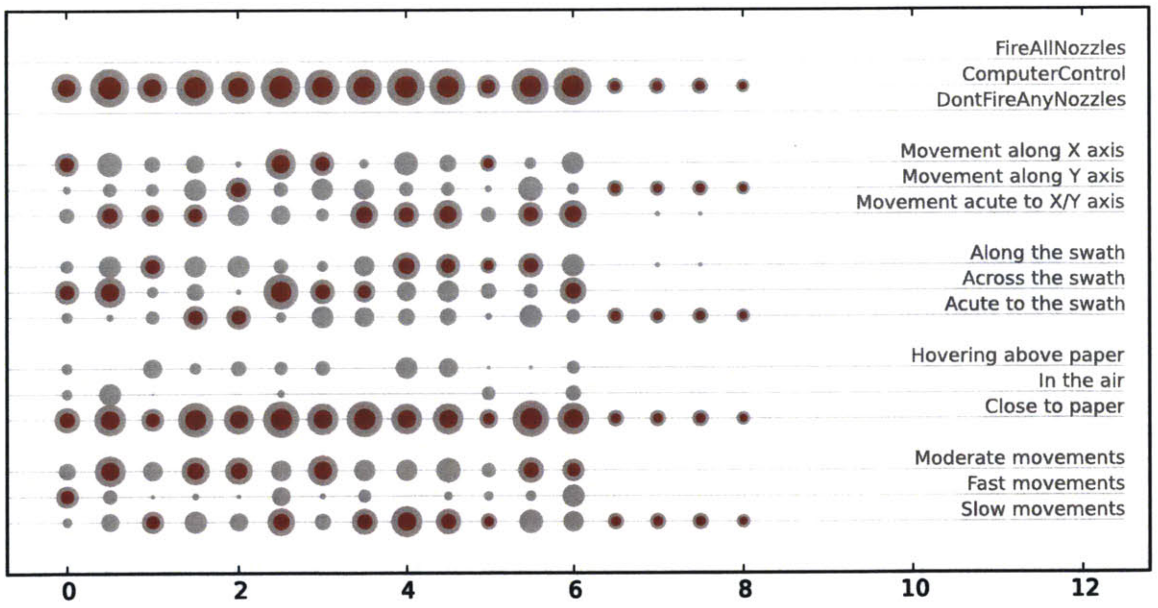

Figure 3-29: Top: Amit's print. Top right: Visualization of handset position data. Bottom: Visualization of usage data.

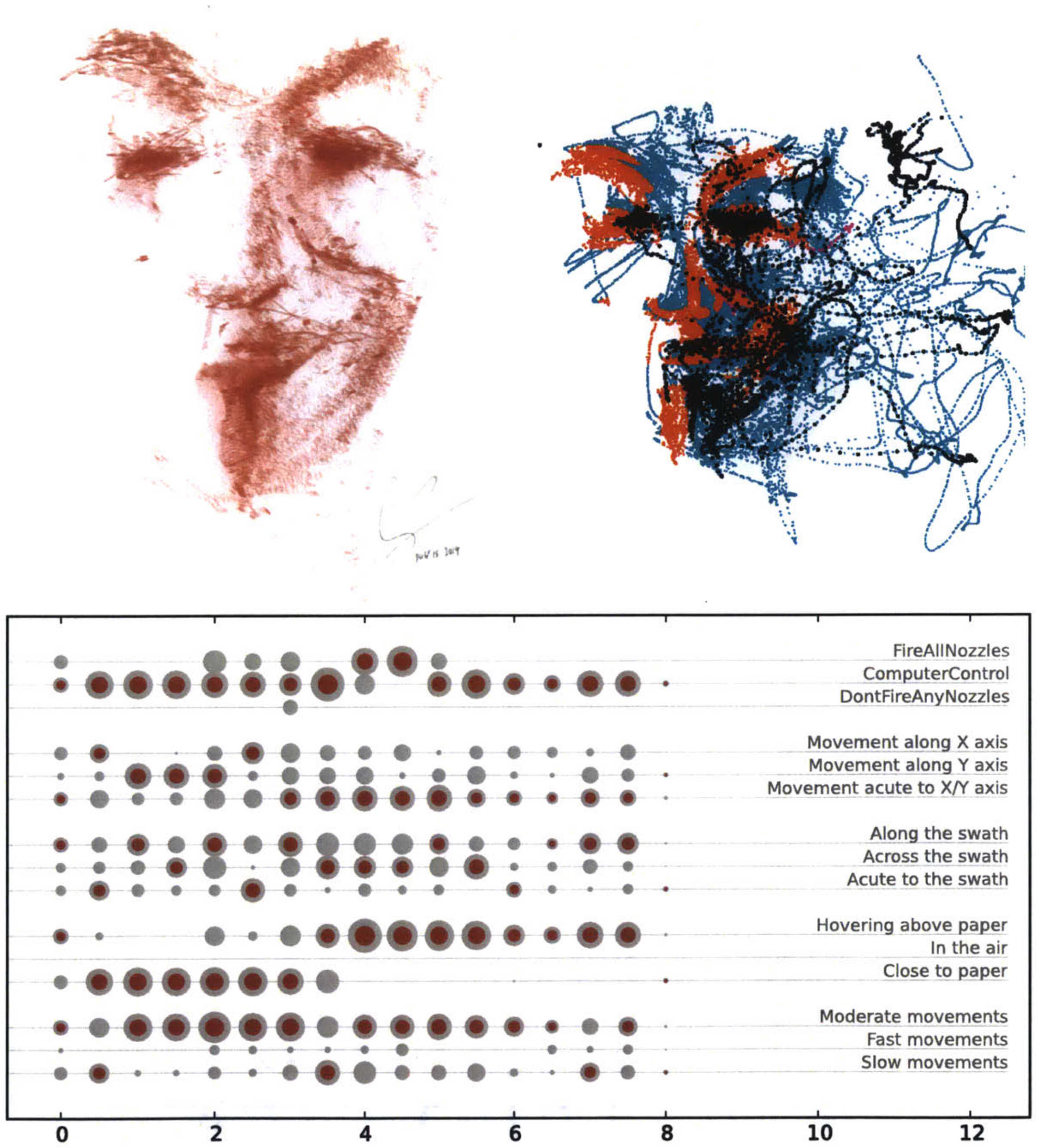

Figure 3-30: Top: Nan's print. Top right: Visualization of handset position data. Bottom: Visualization of usage data.

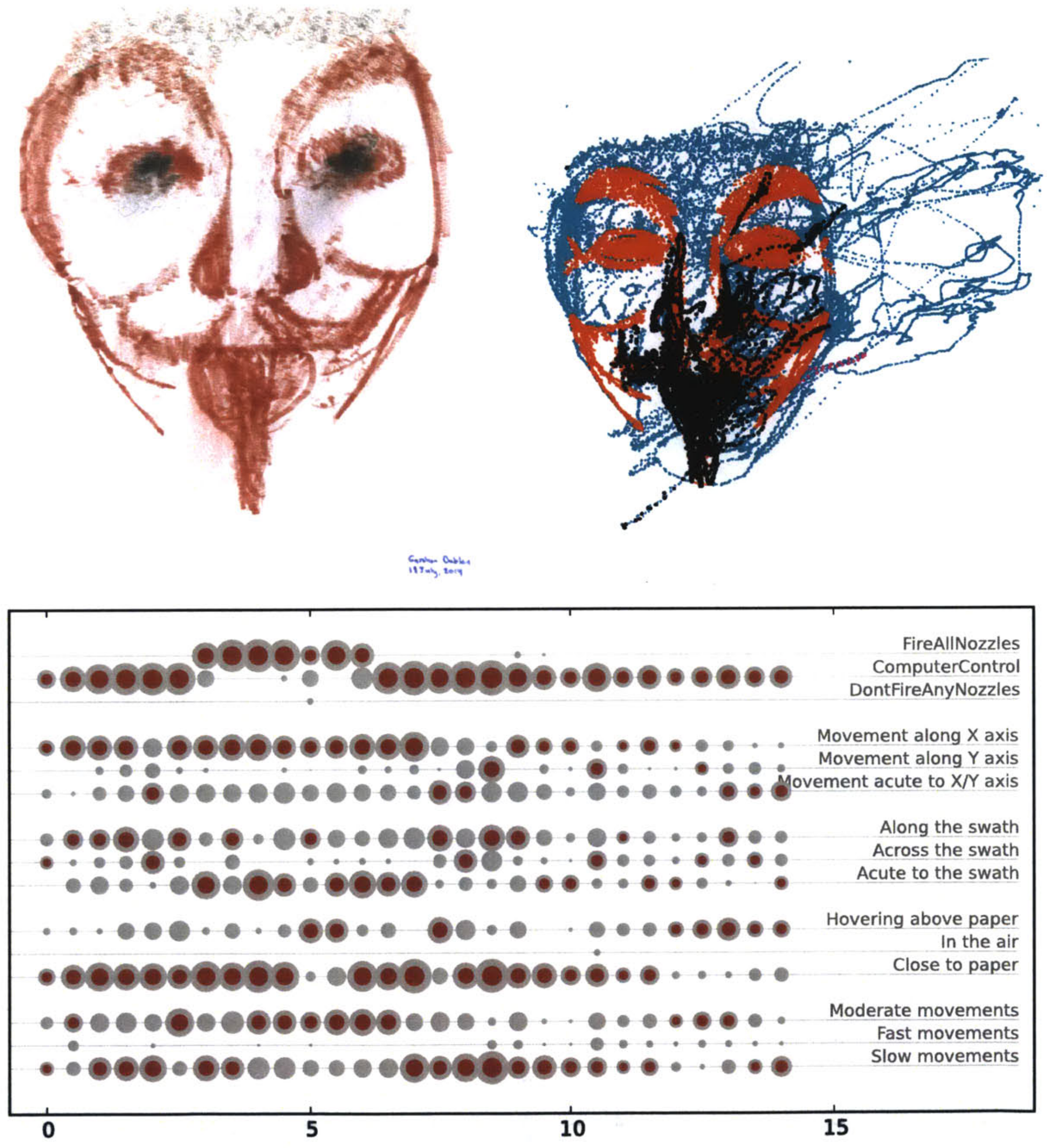

Figure 3-31: Top: Gershon's print. Top right: Visualization of handset position data. Bottom: Visualization of usage data.

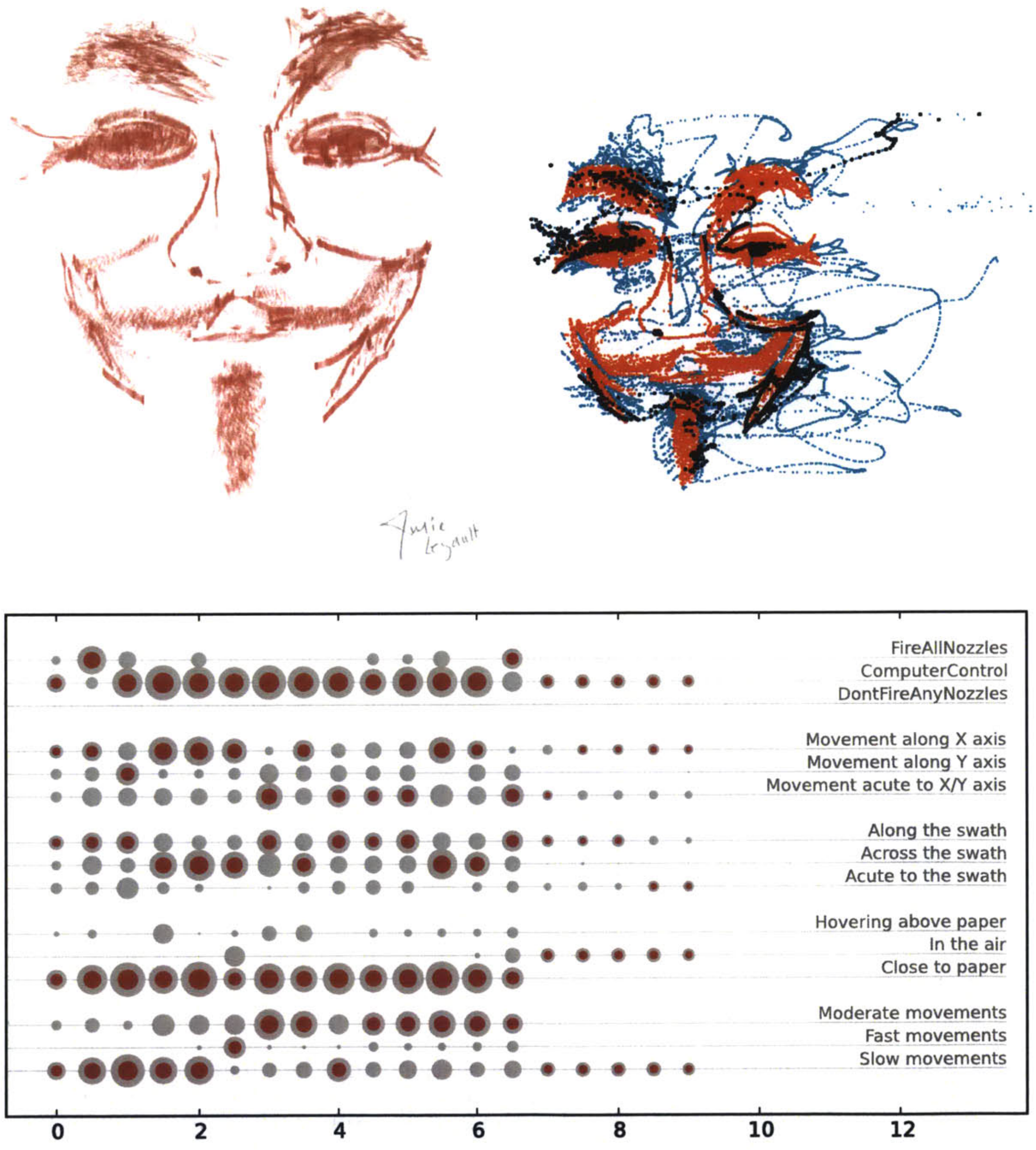

Figure 3-32: Top: Julie's print. Top right: Visualization of handset position data. Bottom: Visualization of usage data.

the introduction of the blank override mode which was made available to the other 5 users.

In her impressions of the tool, Alexis expressed that she would have liked a more ergonomically designed tool that allows her to hold the printhead at an angle with the vertical, allowing her a better visibility of the work surface.

Amit

Amit demonstrated the maximum level of confidence with the tool. This may be due in part to the fact that he himself has created many smart tools similar to Nishanchi. He started with moving the tool with rapid back and forth movements using the automatic mode to create a quick rough version of the computer graphic. He then used the tool in manual override to add the sections in black ink (figure 3-29).

Nan

Nan used the automatic mode in slow, long movements to find some key areas of the figure: eyes, nose, and the goatee. Then, she used the tool in manual override mode to create the appearance a side-lit portrait using key areas from the computer image (figure 3-30).

Gershon

Gershon used the tool to discover outlines of sections and then manually filled those areas using the override mode. He filled in the nostrils using outlines from the original figure, and used a similar technique to join the goatee with the mustache. He used the manual override in quick back and forth movements to create a puffy texture for the hair, which, again, he manually introduced (figure 3-31). Gershon also used the tool as a computer input design, looking at the movement of the inkjet cursor on the screen to guide him while holding the manual override button.

Julie

Julie used the tool in slow, long, curved movements to create long, thick strokes. This may be inspired from Julie's previous work with crayons. (figure 3-32)

Santiago

Santiago used the tool in long, horizontal passes to create quite an accurate version of the computer image on the paper. However, he left some sections empty: the left eye and mustache. He later added his own version of the left eye, a bow, teeth, and a mouth using the manual override in smooth pencil like movements (figure 3-27).

3.10.8 Conclusions

The pilot study with the users was very encouraging. It can be seen how each user was able to use the tool in their own way to express themselves. It can be seen in the final prints that the tool enabled each user to personalize the print by choosing different movement speed, swath angle, and the override buttons. A study involving printing in 3D would reveal more about how the tool can be used by different people in creating prints on curved surfaces.

3.11 Printing in 3D

3.11.1 Printing decorative patterns

The device was used to print a pattern on a large, wooden, hemispherical IKEA bowl spray painted with a coat of gray primer paint. The CAD model for the bowl was created by using the digitizer mode on Nishanchi to create a point cloud scan of the bowl and the plane holding the bowl (figure 3-33). A 2D design (figure 3-34) was projected on the curved surface of the hemisphere. The surface was split along the design curves and alternating surfaces were printed on the bowl in alternating red and black colors (figure 3-35). Despite a printing rate of 40 frames/second, the print

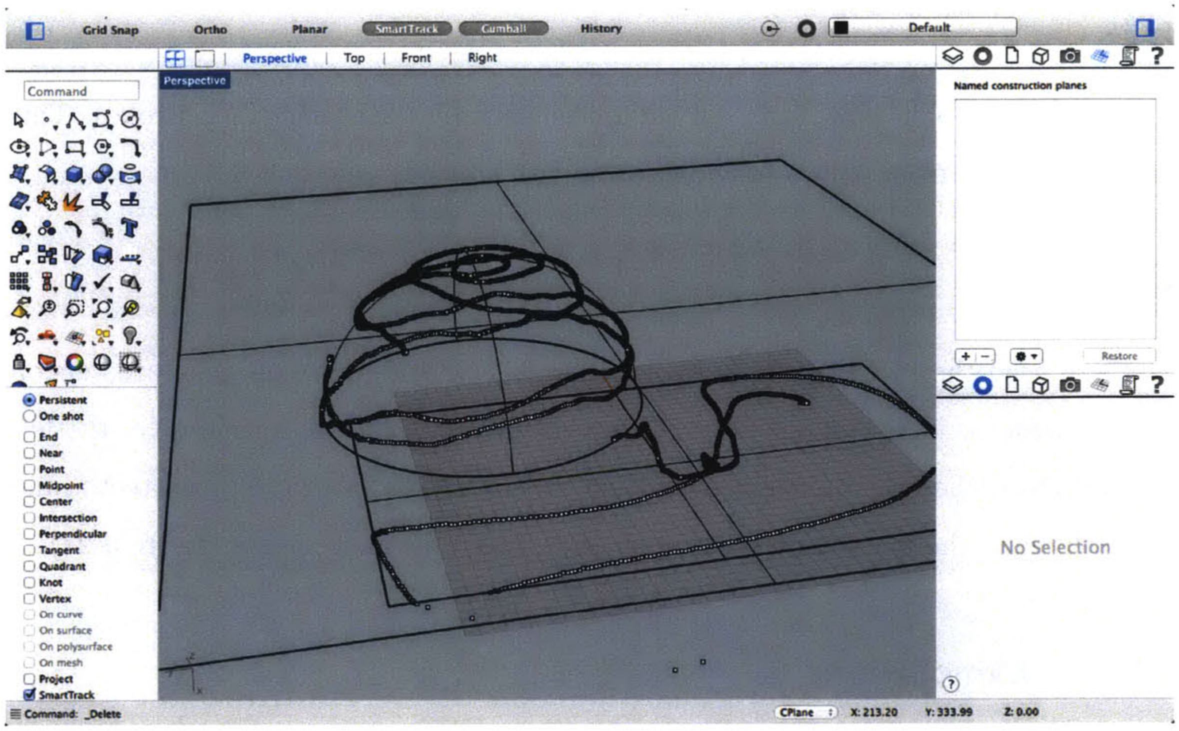

Figure 3-33: A screenshot of the hemispherical model of the bowl and the supporting plane as created in Rhinocerous using the point cloud data.

still took about two hours to finish, which indicates need for improvement in print rate and swath width.

3.11.2 Printing CAD parameters

The system was used to mate an IKEA bowl to the sculpture shown in figure 3-37 and to create a hemispherical base for it. Again, the bowl was input into Rhinoceros software using the digitizer. The lower section of the sculpture was represented as a cube, and the intersection curve between the cube and the bowl was computed (figure 3-38). The Nishanchi system was then used to transfer the intersection curve onto the bowl figure 3-39. The bowl was cut along the lines using a handsaw (figure 3-40). The resulting cut fits the sculpture snugly. Further, as expected, the part of the bowl that was removed by cutting also fits the inside of the yanien sculpture. This example is in line with the motivation behind creating Nishanchi (section 3.1): it shows how the Nishanchi system could be used to output CAD information to the workpiece.

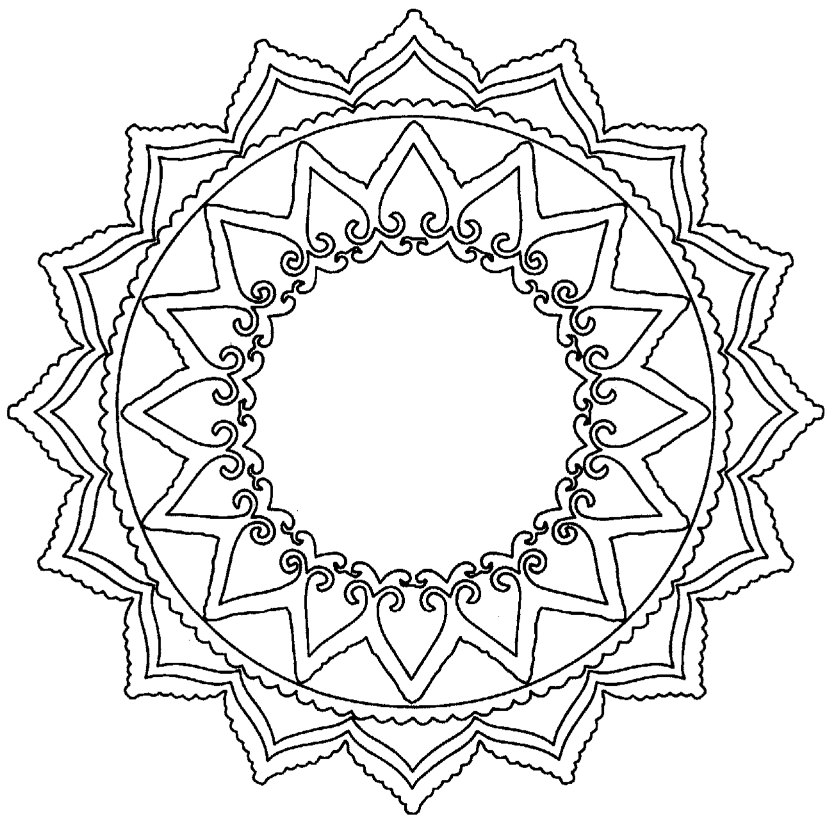

Figure 3-34: The 2D vector art used to render printed surfaces on the bowl.

3.11.3 Impressions

The integration with CAD met all the design objectives laid out for the design of the device. An object with unknown geometrical parameters was rendered with a CAD design using the Nishanchi system. While extensive experiments need to be done to estimate the true resolution and accuracy of prints, the system seemed to perform as accurately as the tracking system, which is about 1mm. In the first example, the system proved to be useful in rendering a decorative pattern on the bowl (figure 3-35). In the second example, the system helped create a functional mate between the bowl and another object (figure 3-37). While it took about two hours to create the decorative pattern, it took less than 5 minutes to render the intersection curve on the bowl. This indicates that while the system is capable of creating complex 3D renderings, it is most useful for sparse prints. More extensive tests with printing in 3D would help understand the limits of the workflow and the Nishanchi device, and

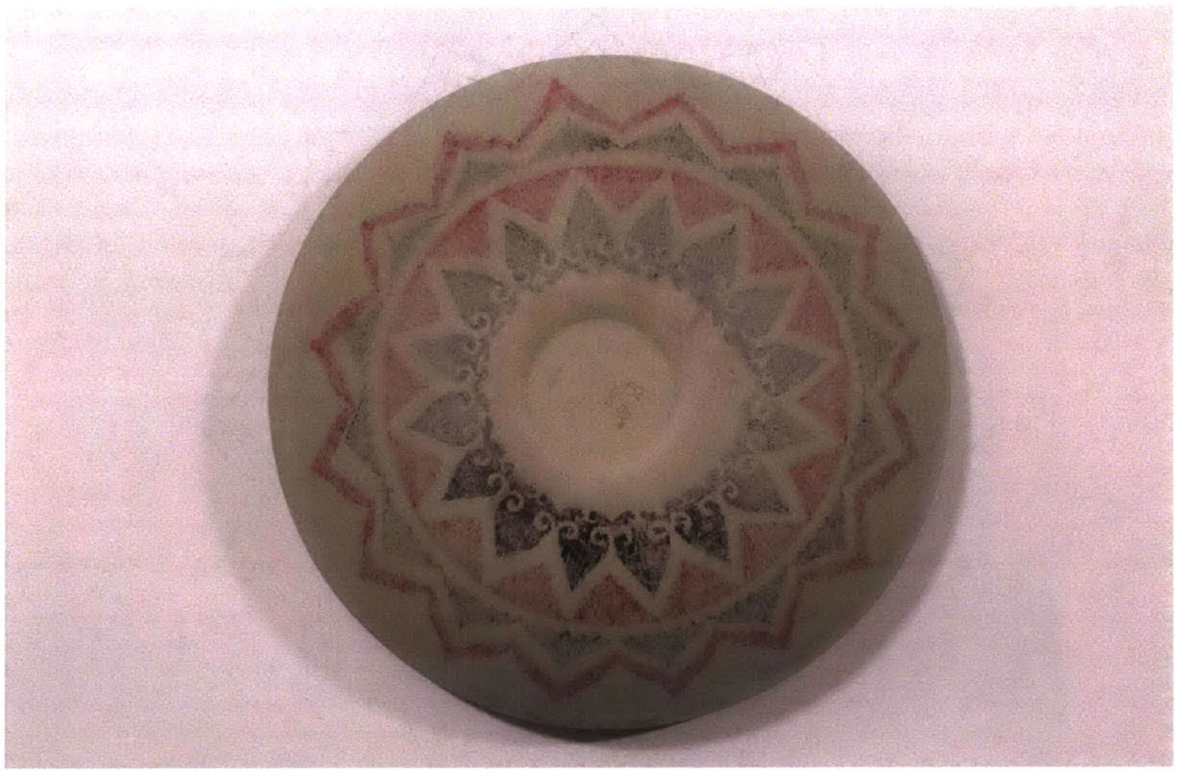
Top view of the printed bowl

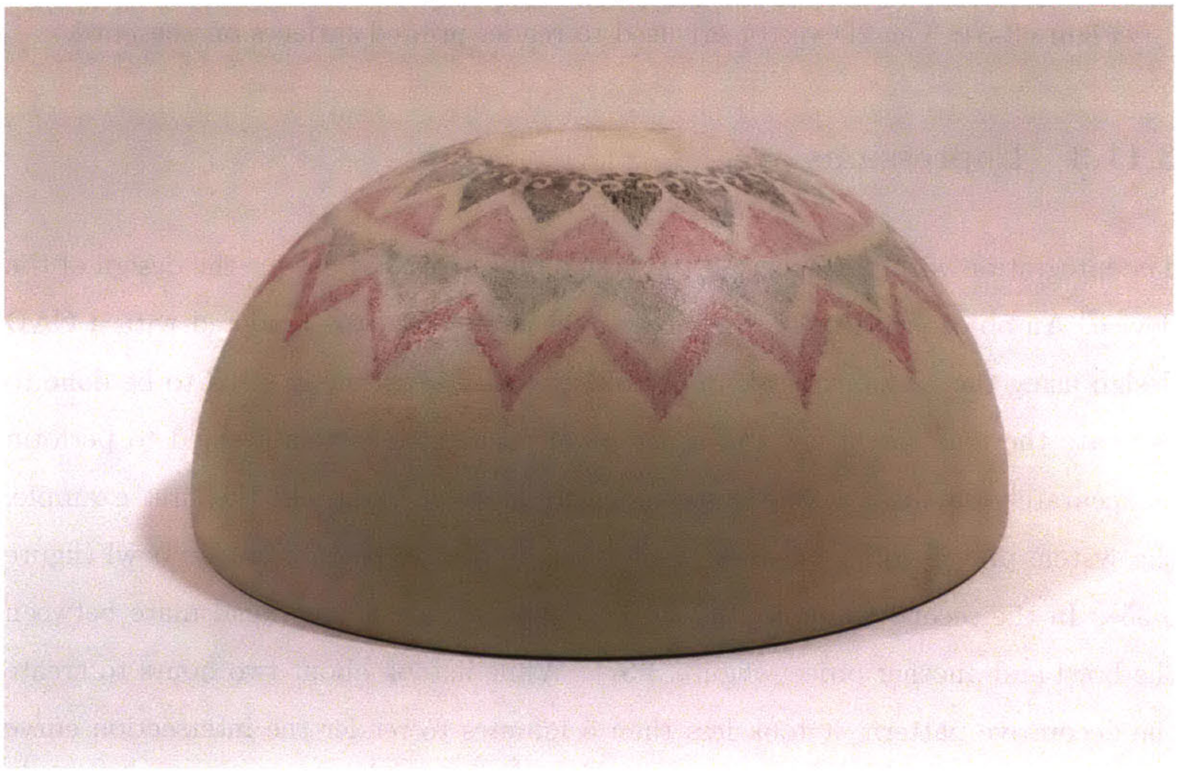
Front view of the printed bowl

Figure 3-35: The bowl printed using Nishanchi with the design derived from figure 3-34.

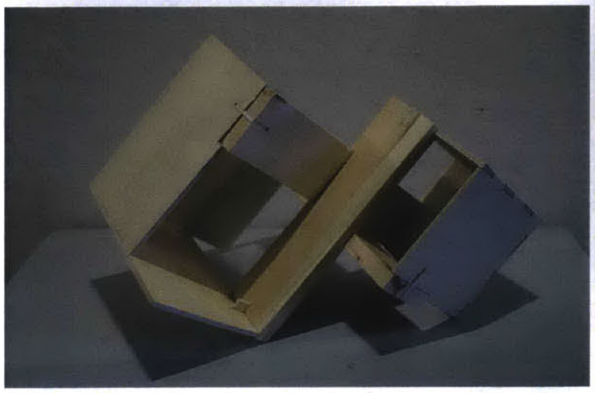

Yanien: A wooden architectural sculpture I had made previously.

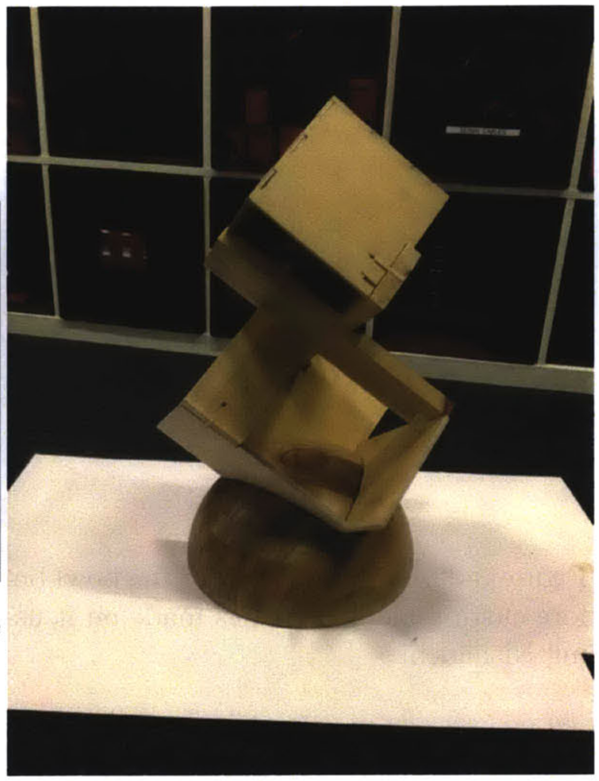

Figure 3-36: The original Yanien sculpture mated with the Ikea bowl as base.

Figure 3-37

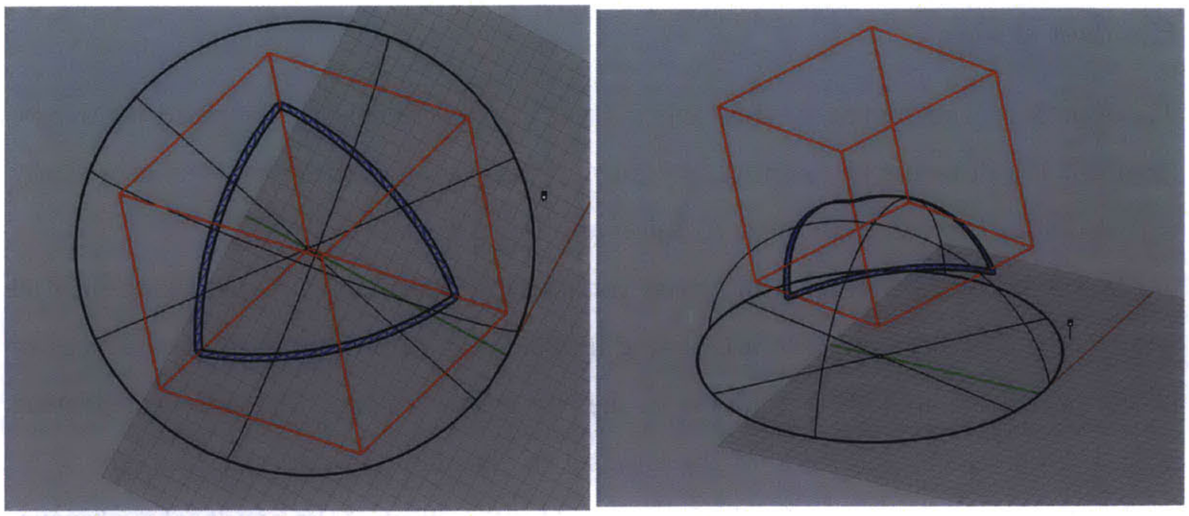

Figure 3-38: Screenshots showing the computation of the intersection curve (blue) between the lower section of the Yanien sculpture (red) and the bowl (black).

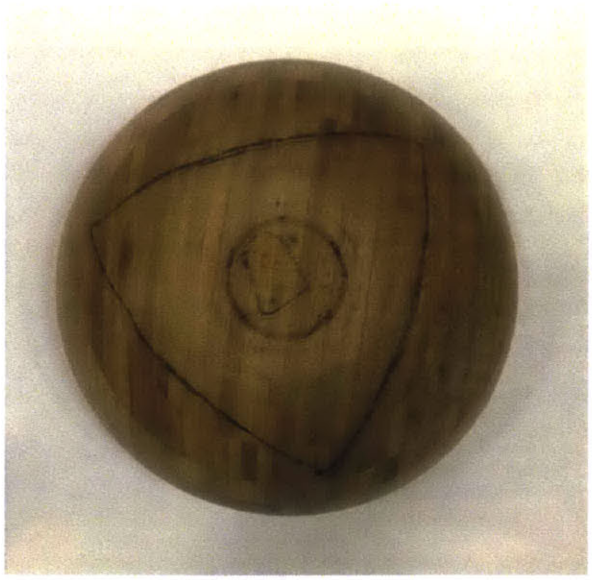

Figure 3-39: A photograph of the bowl before cutting along the lines made on it using Nishanchi.

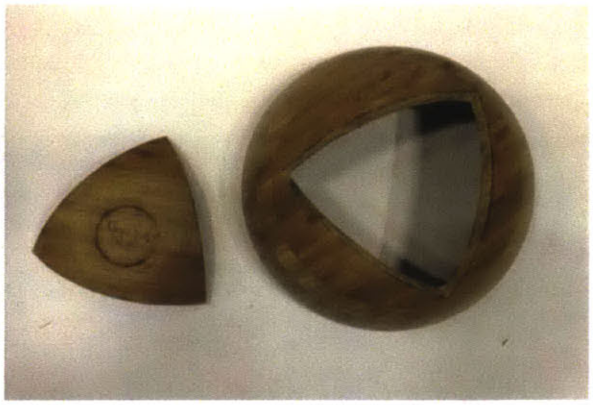

Figure 3-40: After cutting the bowl along the lines.

is part of future work.

3.12 Discussion and future work

3.12.1 Future work

Handset design

The fourth prototype (figure 3-8) was a great improvement over the third prototype (figure 3-19) in terms of usability, weight and performance. However, the user study revealed that several areas need redesign and more work.

As the inkjet printhead is mounted vertically, it obstructs the area being printed on directly. Furthermore, the area being immediately printed upon is in the shadow of the printhead, making it difficult to see the print area from the side. Integrating illumination on the underside of the handset might help alleviate this problem.

In many traditional handtools the area under the affect of the handtool is obvious: the handtool blade, tip, brush or such other extrusion contacts the workpiece at a specific place. However, with inkjet printing, as there is no such obvious contact between the tool and the workpiece, and the user is left to guess where the inkjet nozzles might print to. A visible guide, possibly in the form of a line segment projected on the workpiece, might help.

The fourth prototype (figure 3-8) was intended to be used holding the portruding part of the inkjet printhead itself, as this places the user's fingers closest to the inkjet nozzles. However, in the user study it was found that this holding position is not comfortable over extended use.

Software

The most time consuming computation for the 3D software is the nozzle ray intersection with the 3D object representation, to determine if the nozzle needs to be fired and to determine the ink value for the location. A mesh representation allows realtime performance on medium mesh sizes (about 1000 triangles). However, this implementation searches for the nozzle-triangle intersection over all triangles separately for each nozzle. For future work, the order in which the mesh triangles are searched could instead be computed based on the first nozzle intersection for subsequent nozzle trajectory intersections. For most cases, this would lead to the triangle search stopping within the first few triangles, thereby speeding up the overall computation for trajectory mesh intersections over all the nozzles. Alternatively, another approach would be UV mapped textures. Furthermore, some of these routines could be written with libraries like CUDA to use the GPU (Graphics Processor Unit) to speed up computations.

Inkjet printing system

The inkjet printing system used in this work is the HP C6602. It was chosen for its easy interface, however, it is quite primitive, with a 3.175mm swath and a resolution of 96dpi. The user study revealed that the small swath size limits the effective print speed. Replacing the inkjet printing system with an inkjet cartridge with a larger swath size is recommended.

Chapter 4

Summary and conclusions

In this work, I presented two smart handtools, BoardLab and Nishanchi, with the objective of proposing smart handtools that allow a user to maintain a more seamless connection between the computer and the workpiece. The design process and the details of construction of the final prototypes for both projects are presented. In comparison with Nishanchi, BoardLab has a relatively straightforward usecase, so a formal user study to understand how users would use BoardLab creatively was not conducted. User impressions were collected for Nishanchi for 6 users and it was observed how the tool enabled them to express themselves in the way they chose to use the tool. The user study involved creating a 2D print; this allowed for observing tool usage while avoiding the complications of making prints in 3D. I also used Nishanchi to print a pattern on a hemispherical bowl. This demonstrates the tool's ability to print in 3D and to work interactively with Rhinoceros 3D CAD software.

4.1 Learnings

Some specific learnings from these explorations are detailed in the following sections.

4.1.1 Workpiece re-registration

Workpiece registration and re-registration becomes important with handtools, especially because the workpiece may be removed for some other operations and then brought back into the work environment. A tool or mode to collect data for re-registration becomes very useful. In the case of BoardLab, the probe tip itself can be used for this. BoardLab was also equipped with a registration mode that computes the position and orientation of the PCB using the least squares method automatically. Conversly, another tracking fixture can be attached to the board.

4.1.2 Software framework

The software design was approached in different ways for both projects. The software for BoardLab was written to run independently of the EDA software, with the only connection with the Eagle software being the schematic and PCB layout files. While this approach saves the effort it would have taken to understand the APIs for the EDA software, it also removes the possibilities that a full EDA package would have afforded.

The software for Nishanchi was written completely as a part of Rhinoceros in the form of a Rhinoceros plugin. This allows Nishanchi device data to be processed directly using Rhinoceros primitive functions (for example pointcloud fitting). However, the Rhinoceros plugin environment does not allow for continuous polling of the serial port without blocking the UI.

Based on these experiences, an approach that integrates with CAD for functionality, while handling low-level hardware access from outside the CAD software, is recommended.

4.2 Conclusions

As a medium to express thoughts and ideas, CAD (Computer Aided Design) allows for a large expansive canvas. The information in this medium, however, also gets locked

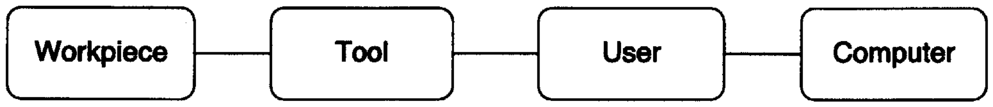

Figure 4-1: Diagram showing simplified information flow in a traditional hand fabrication workflow using CAD. The user mediates the flow of information between the computer and the tool.

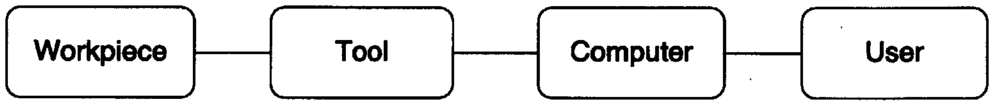

Figure 4-2: Diagram showing simplified information flow in a fabrication workflow using CAD and computer controlled automatic machines (for example CNC mill, 3D printer,etc). The computer blocks the user out from engaging in the actual fabrication process.

up behind traditional interfaces when the real physical artifact is being created. This makes it difficult to make changes to the design quickly and iteratively based on understandings gleaned from the process of creating and working with the physical artifact. Figures 4-1 and 4-2 shows the connections between the user, the computer, the tool and the workpiece in this case. While we can work our way around this by dividing the process of creation into distinct phases of design and realization, this division comes at the cost of freedom of thought and expression. Handtools have allowed humans a high-bandwidth connection with the workpiece for a long time. The smart handtools that I have presented build upon this connection by including into the tool a computer that, is aware of the state of the tool and the task at hand. Figure 4-3 shows the new organization of the tool, the user, the computer and the workpiece.

In making both of these handtools, the objective was to create a way for the creator to include the computer in the making and designing process without distracting from

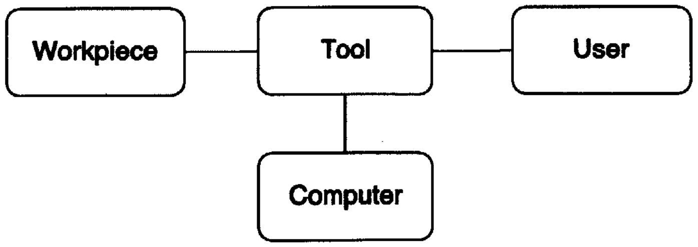

Figure 4-3: Diagram showing the new simplified information flow. The smart tool self-mediates the flow of information to and from the computer.

the object of creation: the workpiece. While creating the base for the Yanien sculpture (figure 3-37), I had the option of executing the cut in a manner that differed from the print made by Nishanchi. While printing the decorative pattern on the bowl (figure 3-35), I had the freedom to leave out a section if I wanted to, add spontaneous color, or to render a section with a darker shade. While making measurements and introspections with BoardLab, I had the freedom to choose where I made the measurement or the introspection. I believe that this freedom allows one to include beautiful non-linear details in the workpiece – details often inspired by the material and the workpiece itself, and not fully or at all anticipated when the CAD model was created. The fact that this freedom also comes with the mathematical structure of computation, programmability, and simulation, might allow the creator to take even higher flights of thought and creativity.

Bibliography

[1] A. Zoran, R. Shilkrot, and J. Paradiso, "Human-computer Interaction for Hybrid Carving," in *Proceedings of the 26th Annual ACM Symposium on User Interface Software and Technology*, ser. UIST '13. New York, NY, USA: ACM, 2013, pp. 433–440. [Online]. Available: http://doi.acm.org/10.1145/2501988.2502023

[2] A. Zoran and J. A. Paradiso, "FreeD: a freehand digital sculpting tool," in *Proceedings of the SIGCHI Conference on Human Factors in Computing Systems.* ACM, 2013, pp. 2613–2616.

[3] A. Zoran, R. Shilkrot, P. Goyal, P. Maes, and J. A. Paradiso, "The wise chisel: The rise of the smart handheld tool," *IEEE Pervasive Computing*, vol. 13, no. 3, pp. 48–57, 2014.

[4] I. E. Sutherland, "Sketch Pad a Man-machine Graphical Communication System," in *Proceedings of the SHARE Design Automation Workshop*, ser. DAC '64. New York, NY, USA: ACM, 1964, pp. 6.329–6.346. [Online]. Available: http://doi.acm.org/10.1145/800265.810742

[5] "Wacom tablets and pens," http://www.wacom.com, accessed: 2014-07-25.

[6] "Anoto digital pens," http://www2.anoto.com/digital-pens-1.aspx, accessed: 2014-07-25.

[7] H. Kim, S. Kim, B. Lee, J. Pak, M. Sohn, G. Lee, and W. Lee, "Digital Rubbing: Playful and Intuitive Interaction Technique for Transferring a Graphic Image Onto Paper with Pen-based Computing," in *CHI '08 Extended Abstracts on Human Factors in Computing Systems*, ser. CHI EA '08. New York, NY, USA: ACM, 2008, pp. 2337–2342. [Online]. Available: http://doi.acm.org/10.1145/1358628.1358680

[8] J. Yamaoka and Y. Kakehi, "dePEDd: Augmented Handwriting System Using Ferromagnetism of a Ballpoint Pen," in *Proceedings of the 26th Annual ACM Symposium on User Interface Software and Technology*, ser. UIST '13. New York, NY, USA: ACM, 2013, pp. 203–210. [Online]. Available: http://doi.acm.org/10.1145/2501988.2502017

[9] K. Ryokai, S. Marti, and H. Ishii, "I/O Brush: Drawing with Everyday Objects As Ink," in *Proceedings of the SIGCHI Conference on Human Factors*

in Computing Systems, ser. CHI '04. New York, NY, USA: ACM, 2004, pp. 303–310. [Online]. Available: http://doi.acm.org/10.1145/985692.985731

[10] P. Vandoren, L. Claesen, T. Van Laerhoven, J. Taelman, C. Raymaekers, E. Flerackers, and F. Van Reeth, "FluidPaint: An Interactive Digital Painting System Using Real Wet Brushes," in *Proceedings of the ACM International Conference on Interactive Tabletops and Surfaces*, ser. ITS '09. New York, NY, USA: ACM, 2009, pp. 53–56. [Online]. Available: http://doi.acm.org/10.1145/1731903.1731914

[11] P. Vandoren, T. Van Laerhoven, L. Claesen, J. Taelman, C. Raymaekers, and F. Van Reeth, "IntuPaint: Bridging the gap between physical and digital painting," in *Horizontal Interactive Human Computer Systems, 2008. TABLETOP 2008. 3rd IEEE International Workshop on*, Oct 2008, pp. 65–72.

[12] B. Baxter, V. Scheib, M. C. Lin, and D. Manocha, "DAB: Interactive Haptic Painting with 3D Virtual Brushes," in *Proceedings of the 28th Annual Conference on Computer Graphics and Interactive Techniques*, ser. SIGGRAPH '01. New York, NY, USA: ACM, 2001, pp. 461–468. [Online]. Available: http://doi.acm.org/10.1145/383259.383313

[13] "Creaform Handheld 3D Scanner," http://www.creaform3d.com/en, accessed: 2014-07-25.

[14] H. Song, F. Guimbretière, and H. Lipson, "The ModelCraft Framework: Capturing Freehand Annotations and Edits to Facilitate the 3D Model Design Process Using a Digital Pen," *ACM Trans. Comput.-Hum. Interact.*, vol. 16, no. 3, pp. 14:1–14:33, Sep. 2009. [Online]. Available: http://doi.acm.org/10.1145/1592440.1592443

[15] A. Rivers, I. E. Moyer, and F. Durand, "Position-correcting Tools for 2D Digital Fabrication," *ACM Trans. Graph.*, vol. 31, no. 4, pp. 88:1–88:7, Jul. 2012. [Online]. Available: http://doi.acm.org/10.1145/2185520.2185584

[16] J. Chan, T. Pondicherry, and P. Blikstein, "LightUp: An Augmented, Learning Platform for Electronics," in *Proceedings of the 12th International Conference on Interaction Design and Children*, ser. IDC '13. New York, NY, USA: ACM, 2013, pp. 491–494. [Online]. Available: http://doi.acm.org/10.1145/2485760.2485812

[17] D. Merrill and P. Maes, "Augmenting Looking, Pointing and Reaching Gestures to Enhance the Searching and Browsing of Physical Objects," in *Proceedings of the 5th International Conference on Pervasive Computing*, ser. PERVASIVE'07. Berlin, Heidelberg: Springer-Verlag, 2007, pp. 1–18. [Online]. Available: http://dl.acm.org/citation.cfm?id=1758156.1758158

[18] J. R. R. Louis B. Rosenberg, "Component Position Verification Using a Probe Apparatus," Patent US 6 195 618, 02 27, 2001.

[19] F. Raab, E. Blood, T. Steiner, and H. Jones, "Magnetic position and orientation tracking system," *Aerospace and Electronic Systems, IEEE Transactions on*, vol. AES-15, no. 5, pp. 709–718, Sept 1979.

[20] O. Sorkine, "Least-Squares Rigid Motion Using SVD," *Technical notes*, vol. 120, p. 3, 2009.

[21] "Hp 34401a user's guide, chapter 4: Remote interface reference, pages 105-173," https://www.physics.rutgers.edu/ugrad/327/HP34401.pdf, pp. 105–173, accessed: 2014-07-05.

[22] "PrintBrush 4X6 Handheld Printer," http://www.printdreams.com, accessed: 2014-07-01.

[23] N. C. Lewis, "Inkshield," http://nicholasclewis.com/projects/inkshield/, accessed: 2014-07-01.

[24] "Data Throughput, Latency and Handshaking," Application Note. [Online]. Available: http://www.ftdichip.com/Support/Documents/AppNotes/AN232B-04_DataLatencyFlow.pdf

[25] "FT8U232/FT8U245 Devices Latency and Data Throughput," Application Note. [Online]. Available: http://www.ftdichip.com/Support/Documents/AppNotes/AN232-04.pdf

[26] A. Zoran, R. Shilkrot, S. Nanyakkara, and J. Paradiso, "The Hybrid Artisans: A Case Study in Smart Tools," *ACM Trans. Comput.-Hum. Interact.*, vol. 21, no. 3, pp. 15:1–15:29, Jun. 2014. [Online]. Available: http://doi.acm.org/10.1145/2617570